Bollettino di Geofisica Teorica ed Applicata Vol. 55, n. 2, pp. 433-468; June 2014
DOI 10.4430/bgta0090

Seismic hazard estimates for the area of Pylos and surrounding region (SW Peloponnese) for seismic and tsunami risk assessment

D. Slejko, M. Santulin and J. Garcia

Ist. Nazionale di Oceanografia e di Geofisica Sperimentale, Trieste, Italy

(Received: January 14, 2011; accepted: April 4, 2013)

ABSTRACT This paper summarizes the activity developed for the seismic hazard assessment of the Pylos broader area in the framework of the SEAHELLARC project. In addition to the geological, geophysical, and seismological information available in literature, the definition of the seismogenic zones, applied for seismic hazard assessment, was based on the results of the active and passive seismic experiments performed during this project. In particular, a new earthquake catalogue covering the period 550 B.C. to 2009 was compiled. A logic tree with 24 branches has been constructed: it consists of two zonations, two approaches for the seismicity model definition, two methods for maximum magnitude estimate, and four attenuation relations for horizontal peak ground acceleration (*PGA*). One of the zonations used was specially developed for the Pylos broader area during the SEAHELLARC project: it is notably different from the national model while the national model, with marginal modifications, was accepted for the seismic sources far away from the study area. The results are presented in forms of separate seismic hazard maps of the broader Pylos area, seismic hazard curves and uniform hazard response spectra for Pylos town, for different soil types, suitable for a seismic risk assessment. In addition, a soil seismic hazard map has been elaborated for the Pylos area: it takes into consideration the specific soil types at any sites. Pylos is characterized by a high seismic hazard (*PGA* around 0.5 g for a 475-year return period on rock), remarkably lower, anyway, than that of the Ionian islands. The widespread presence of rock around the town does not suggest the possibility of unexpected high ground motions. The identification of the possible earthquakes capable of generating tsunamis dangerous for Pylos town has been based on the deaggregation of the hazard results and considerations on the seismic faults identified in the Ionian Sea.

Key words: SEAHELLARC, PSHA, seismogenic zones, soil types, western Peloponnese.

1. Introduction

Seismic risk represents a major threat for Greece and this is particularly important for the Ionian islands [Corfu, Lefkas, Cephalonia, and Zakynthos; see e.g., Papoulia and Slejko (1997)] and the coastal border of western Hellenic Arc, where earthquakes, among the largest ones known in the Mediterranean Sea, have occurred in the past (Fig. 1). In fact, the western border of Peloponnese

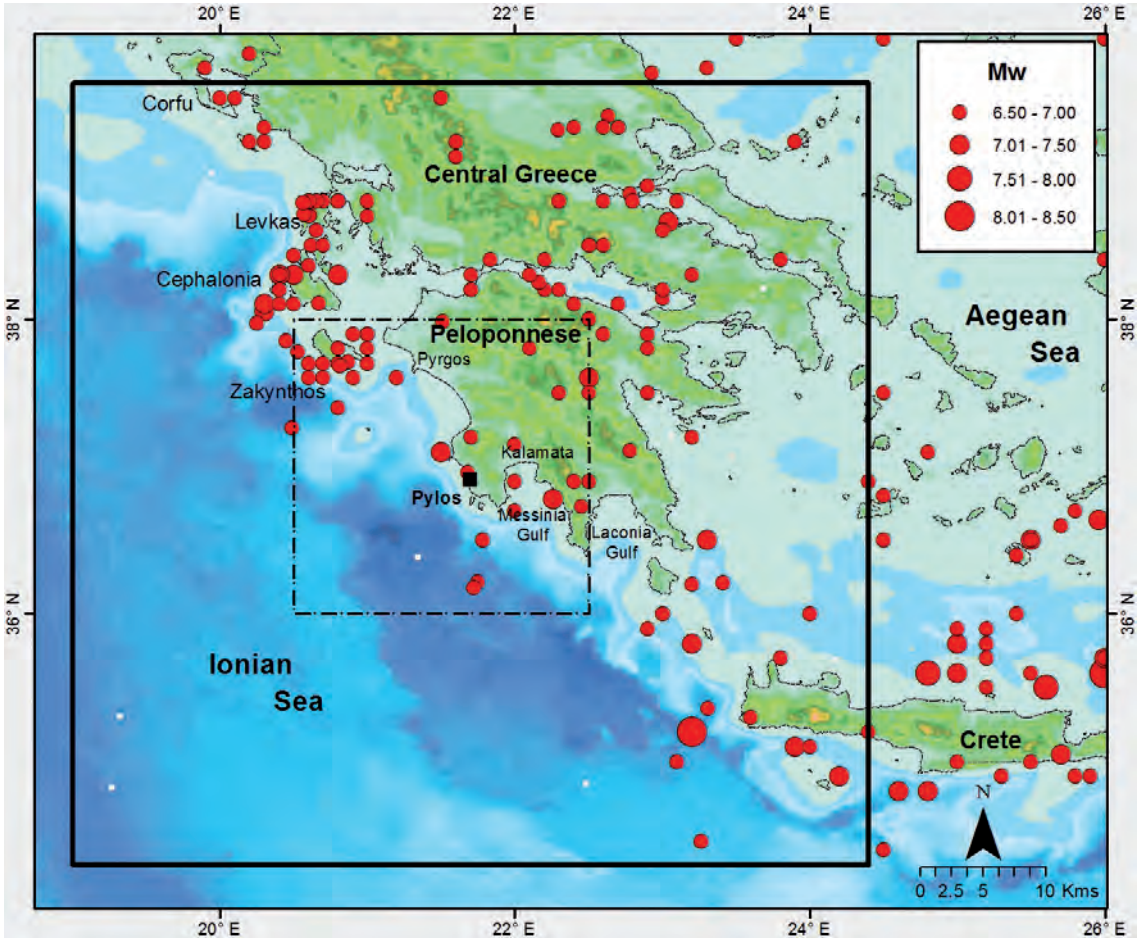

Fig. 1 - Index map of the study region: the large square indicates the area where seismogenic zones are defined (study region), the small square shows the area where seismic hazard for rock, stiff soil, and soft soil has been assessed (Pylos broader area). The epicentres of the earthquakes with $M_w \geq 6.5$ in the SEAHELLARC catalogue are reported as well.

has been repeatedly affected by large magnitude earthquakes that caused severe destruction and human losses [i.e., the M_S 7.3 Filiatra in 1886, the M_S 6.5 Zante-Keri in 1893, the M_S 6.5 Kyparissia in 1899, the M_S 7.0 Pylos in 1947, and the M_S 6.6 Gargaliani in 1997; Papazachos and Papazachou (1997)]. Some of the largest tsunamis of the Mediterranean Sea have been reported along the western coast of Peloponnese in association with some large earthquakes (i.e., in 365, 1630 and 1866), while local earthquakes have induced even strong tsunamis (Papadopoulos *et al.*, 2010).

The Peloponnese is part of the Aegean microplate, which is moving SW-wards (McClusky *et al.*, 2000) overriding the African plate along the Hellenic subduction zone, and sliding past the Apulian platform along the dextral strike-slip Cephalonia transform fault to the west (Scordilis *et al.*, 1985; Papazachos *et al.*, 1998). The Cephalonia transform fault links the subduction boundary to the continental collision and plays a key role in the geodynamic complexity of this region (Louvari *et al.*, 1999). The Pylos broader area is thus located on the overriding crust of the subduction zone, not far from the Cephalonia transform fault zone, to the north, one of the

most seismically active regions of the Mediterranean. A detailed description of the main tectonic features in the study region can be found in SEAHELLARC Working Group (2010).

Seismic hazard studies have been widely developed for Greece [see Papazachos *et al*. (1993) and references therein] as well as for the western coast of Peloponnese and for the Ionian islands [see SEAHELLARC Working Group (2010) and references therein]. Recently, Weatherill and Burton (2010) applied Monte Carlo simulations to assess seismic hazard for whole Greece and estimated an expected horizontal peak ground acceleration (*PGA*) with a 475-year return period between 0.4 and 0.5 g for the western coast of Peloponnese while the SEAHELLARC Working Group (2010) produced some preliminary estimates specifically for the Pylos broader area. In their maps, the highest ground shaking refers to the Island of Zakynthos (*PGA* values larger than 0.96 g) and ground motions between 0.56 and 0.64 g characterize the coast around Pylos.

Benefiting from the analyses done during the first stage of the SEAHELLARC project (SEAHELLARC Working Group, 2010), a more complex seismic hazard assessment has been developed by using the logic tree approach (Kulkarni *et al*., 1984; Coppersmith and Youngs, 1986), where alternative options can be considered and, consequently, the uncertainties related to the computation can be evaluated.

Aim of the present paper is to summarize the choices done and the computations developed to reach robust seismic hazard estimates for the Pylos broader area and to show the final seismic hazard estimates of the SEAHELLARC project (Papoulia *et al*., 2014).

2. The SEAHELLARC earthquake catalogue

For the needs of the seismic hazard assessment of the Pylos broader area, an earthquake catalogue of western Greece (geographical corner co-ordinates from 34.00° N to 40.00° N and from 19.00° E to 27.00° E) covering the time interval from the 6th century B.C. up to December 2009 was prepared by the National Observatory of Athens (NOA) in the framework of the present project (Papadopoulos *et al*., 2014).

For the historical part, that is up to 1899, the catalogue is based on the catalogue of Papazachos and Papazachou (1997), extensively revised and integrated by NOA on the basis of the recent literature (Papadopoulos *et al*., 2000, 2014; Papadopoulos and Plessa, 2001; Papadopoulos and Vassilopoulou, 2001). For the period 1900 to 1999, the catalogue of the University of Thessaloniki has been adopted, which is nearly identical with that of NOA but it is more homogeneous, particularly for the magnitudes (expressed in terms of M_S), and the instrumental locations of NOA have been taken for the last years (till 2009).

The catalogue constructed by NOA and used in the present study (hereafter SEAHELLARC catalogue) derives, then, from three data files: 1) the revised version of the historical earthquake catalogue of Greece (Papazachos and Papazachou, 1997) for the period between 550 B.C. to 1899, 2) the Thessaloniki earthquake catalogue of Greece, for the period from 1900 to 1999, and 3) the NOA earthquake locations from 2000 to December 2009 (see additional details in SEAHELLARC Working Group, 2010).

The accuracy of the epicentral location is less than 30 km (Papazachos and Papazachou, 1997) for the historical period and variable with time from 30 to 10 km after 1900 (Vlastos *et al*., 2002). The depth estimate is more problematic, especially using macroseismic data: only a separation

between shallow, intermediate, and deep events is, then, generally feasible. These uncertainties slightly influence the hazard estimates that are based on wide seismogenic zones and large ranges of focal depths.

Magnitude is a crucial parameter for hazard assessment and a detailed analysis was conducted on the SEAHELLARC catalogue. Considerations about magnitude uncertainties can be found in Papazachos *et al*. (2002). In summary, three time segments can be considered for the SEAHELLARC catalogue: the historical period (pre-1911), where an M_S referring mainly to large events (M_S larger than 6) is given and it can be considered equivalent to M_W (Papazachos and Papazachou, 1997), an early instrumental period (1911-1965), where an M_S referring again mainly to large events is reported and it can be considered again equivalent to M_W (Papazachos and Papazachou, 1997), and a recent instrumental period, where an M_S equivalent to M_W for large events is given and an M_L for small events. For events with an M_S lower than 6, the following relation (Papazachos and Papazachou, 1997) was applied:

$$M_W = 0.56\, M_S + 2.66, \qquad 4.2 \le M_S \le 6.0. \tag{1}$$

It is well known that also low magnitude events contribute to seismic hazard assessment because of their high frequency (Reiter, 1990; Slejko and Rebez, 2002) and as an appreciable number of recent earthquakes (1854 events after the year 2000) in the Pylos broader area remained, anyway, without any magnitude value, it was decided to compute a proxy (M_L*) of M_L for these events using the information available in the NOA bulletins from 2000 to 2009 (i.e., number of stations used in the location procedure) based also on some previous experience for Greek earthquakes. Papazachos *et al*. (2000a), in fact, obtained two scaling laws between number of stations recording the event (*NS*) and M_L for the outer and the inner part of the Hellenic Arc, using the data of International Seismological Centre.

The procedure here developed is simple and it is based on the hypothesis that, if the number of operating stations in Greece has not changed greatly, it is possible to infer an M_L value in a statistical way from the number of stations recording the event. As in Greece the number of operating stations is large enough to support the application of this statistical procedure but has increased notably in the period 2002 to 2004, a normalization procedure [as already proposed by Ambraseys (2003)] has been applied,

$$N_S = \frac{(N_0) \cdot (NS)}{N_R} \tag{2}$$

where N_0 and N_R are, respectively, the number of operating stations in the reference year (2000) and in the year of the studied earthquake; and *NS* and N_S are, respectively, the actual and the normalized number of stations recording the event.

Individual scaling laws were searched for shallow ($h < 30$ km), intermediate ($30 \text{ km} \le h \le 60$ km), and deep ($h > 60$ km) events. As a single correlation between N_S and M_L (considering M_D equivalent to M_L) valid for the entire region presents a large scatter, the study region was subdivided into three zones: the inner part of the Hellenic Arc (Zone 3) and two sectors (with limit offshore the Mani Peninsula) of the outer part (Zone 1 to the NW). Due to the scarcity of data, this subdivision was not possible for the deep events.

After having grouped the events by N_S and M_L, the data of each zone were fitted with a model of the form:

$$M_L = c_1 + c_2 \times \log (N_S) \quad (3)$$

where c_1 and c_2 are the unknown coefficients to be estimated. Successively, considering some high uncertainties obtained especially for some zones (e.g., Zone 3), the median value of M_L for each value of N_S was considered and the data were fitted again using the same regression model of Eq. (3).

The results of the regression analysis are reported in Table 1 and Fig. 2. In spite of the data scattering, similar results were obtained using both approaches (individual M_L values or median ones), with the exception of the case of shallow earthquakes in the inner part of the Hellenic Arc.

Eventually, the results have been considered satisfactory and the magnitude M_L* was computed for all events without a magnitude value of the SEAHELLARC catalogue.

Table 1 - Results of the regression analysis between N_S and M_L. *MR* is the magnitude range, *N* is the number of data and *R* is the correlation coefficient.

Zone	Shallow							
	N	*MR*	All values			Median values		
			c_1	c_2	*R*	c_1	c_2	*R*
1	5366	2.0-4.8	2.283	1.296	0.71	1.955	1.648	0.95
2	1894	1.7-4.6	2.641	1.097	0.63	2.566	1.175	0.91
3	2906	1.4-4.8	2.186	1.091	0.50	1.933	1.465	0.89
Zone	Intermediate							
	N	*MR*	All values			Median values		
			c_1	c_2	*R*	c_1	c_2	*R*
1	512	2.1-4.6	2.399	1.182	0.69	2.029	1.568	0.91
2	434	2.2-4.6	2.470	1.314	0.72	2.456	1.286	0.93
3	724	1.8-4.7	2.399	1.009	0.54	1.906	1.594	0.96
Zone	Deep							
	N	*MR*	All values			Median values		
			c_1	c_2	*R*	c_1	c_2	*R*
All data	134	2.7-4.6	2.081	1.457	0.68	1.888	1.612	0.86

With the aim of having an homogeneous (as possible) M_W for all events, M_L has been transformed into M_W by (Papazachos and Papazachou, 1997):

$$M_W = 0.97\, M_L + 0.58, \qquad 4.5 \le M_L \le 6.0 \quad (4)$$

tentatively extrapolated also to lower values, when necessary.

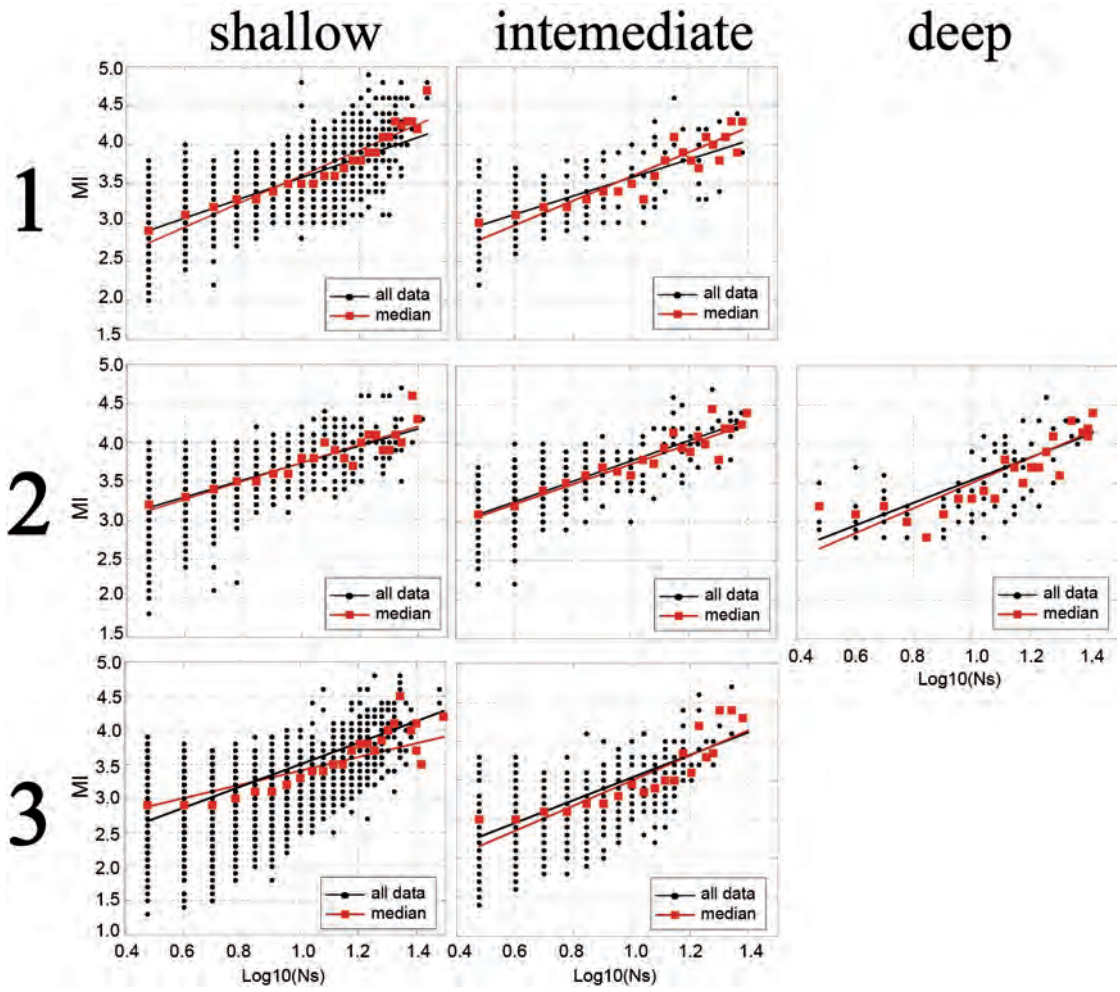

Fig. 2 - Regression curves of M_L vs. N_S for shallow, intermediate and deep earthquakes in zones 1, 2, and 3 (see Table1). The black dots represent the entire data set (the black line is the data interpolation), while the red squares show the median values (the red line is the interpolation of the median values).

The SEAHELLARC catalogue consists, at the end, of 74,787 events with magnitude M_W that occurred from 550 B.C. to December 2009. The minimum magnitude in the catalogue is M_W 1.3, but the catalogue is extremely poor for events before 1400, and almost only earthquakes characterized by an M_W larger than 6 are reported before 1800. An improvement of the data acquisition occurred since 1900, but low magnitude events are reported only after 1964 [see details in SEAHELLARC (2010)]. As already stated, the quality of the location also improved with time and acceptable depth estimates seem to be available only for the last few decades. The catalogue used in the present study differs only slightly from that used by SEAHELLARC Working Group (2010) because it was updated for the last year and a half, some magnitudes of recent events were revised, and magnitude was added to 1718 small events. Consequently, the considerations about its contents (e.g., time distribution, completeness periods for the different magnitude classes, Poisson character, etc.) presented in SEAHELLARC Working Group (2010) can be considered valid also for the present catalogue.

3. The ultimate seismic hazard assessment for the Pylos broader area

As in the preliminary estimates (SEAHELLARC Working Group, 2010), the probabilistic seismic hazard assessment (PSHA) for the Pylos broader region has been done according to the standard approach of Cornell (1968) by using the computer formulation of Ordaz *et al*. (2007). The first elaboration of an earthquake catalogue, in view of its use for a PSHA following the Cornell's (1968) approach, is to eliminate foreshocks and aftershocks. In the present study, the removal of the dependent events was done according to the Gardner and Knopoff (1974) approach: i.e., by applying a space - time window calibrated on Greek seismic sequences (Latoussakis and Stavrakakis, 1992). In such a way, 35,610 dependent events were eliminated from the catalogue and the final data file used for hazard estimates (hereafter Dec-SEAHELLARC catalogue) include 39,177 events with magnitude larger than 1.7.

The quantification of the uncertainties (McGuire, 1977) is a crucial point in modern PSHA. Two kinds of uncertainties characterise the results in PSHA: the aleatory variability and the epistemic uncertainty (McGuire and Shedlock, 1981; Toro *et al*., 1997). Aleatory variability is the natural randomness in a process: it is considered in PSHA taking into account the standard deviation of the relation describing the process. Epistemic uncertainty is the scientific uncertainty in the model of the process and it is due to limited data and knowledge: it is considered in PSHA using alternative models. The logic tree approach for PSHA (Kulkarni *et al*., 1984; Coppersmith and Youngs, 1986) has been introduced for quantifying the epistemic uncertainties. Each node of the logic tree represents a specific topic of the calculation (seismogenic source zonation, seismicity model, attenuation model, etc.) and collects a series of alternative models, represented by the different branches of the logic tree. The alternative branches should be independent each other and exhaustive, in the sense that they should represent the complete opinions of the informed scientific community. The final aggregate result (mean value and standard deviation) is obtained by weighting adequately the individual results coming from the different branches [see more discussion in Rebez and Slejko (2004)].

In the present study, a logic tree (Fig. 3) with 24 branches has been constructed: it consists of two zonations [one of national relevance (Papaioannou and Papazachos, 2000): P&P in Fig. 3, and the one specially developed for the Pylos area during the SEAHELLARC project (SEAHELLARC Working Group, 2014): PYL in Fig. 3], two approaches for the seismicity model definition [Slejko *et al*. (1998): HNH in Fig. 3; Albarello and Mucciarelli (2002): A&M in Fig. 3], two methods for maximum magnitude (M_{max}) assessment [the statistical method proposed by Kijko and Graham (1998): K&G in Fig. 3, and a geological one based on the fault length (Wells and Coppersmith, 1994): GEO in Fig. 3], and four ground motion prediction equations (GMPEs) for horizontal *PGA*. Two of the GMPEs [Ambraseys *et al*. (1996): AMB in Fig. 3; Skarlatoudis *et al*. (2003): SKA in Fig. 3] refer to shallow earthquakes [reduced to only one for spectral acceleration (SA)] and the other two are suitable for intermediate and deep events [Youngs *et al*. (1997): YOU in Fig. 3; Atkinson and Boore (2003): A&B in Fig. 3]. In general, the branches are weighted evenly, with the exception of the PYL zonation and the HNH method that are preferred (see the individual weights in brackets in Fig. 3).

All seismic hazard maps refer to horizontal *PGA* with a 475-year return period, standard reference for seismic design. The magnitude scale considered to characterize the seismicity is the moment magnitude, M_W. Calculations have been repeated for rock, stiff, and soft soil.

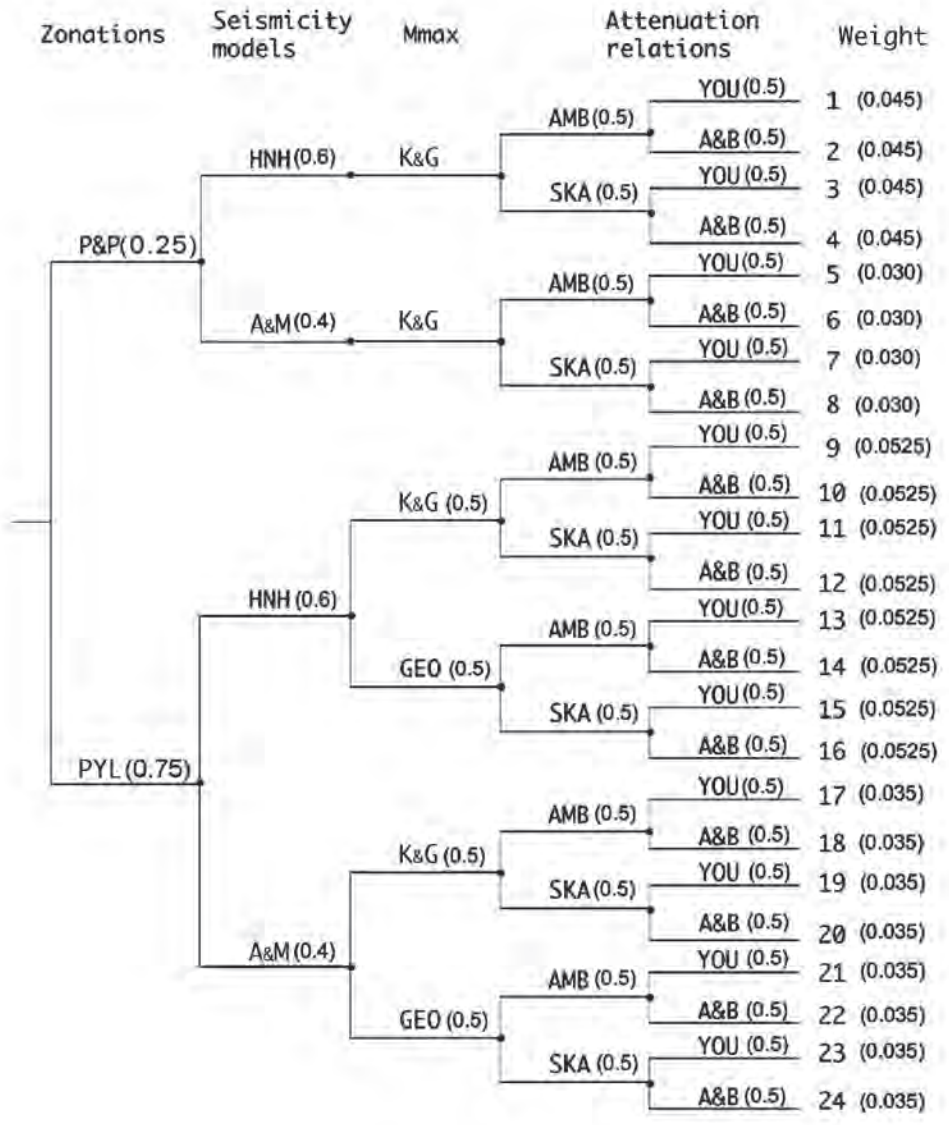

Fig. 3 - Logic tree used for PSHA of the Pylos broader area (see the text for the acronyms).

3.1. The seismogenic zonation

In the standard PSHA, seismic sources are modelled either as seismic lines (faults) or wide seismogenic zones (SZs), where earthquakes can randomly occur. Two seismogenic zonations have been used for the present PSHA, both based on SZs (Fig. 4): they represent different levels of seismotectonic details.

The first seismogenic zonation here considered (Fig. 4a) was proposed by Papaioannou and Papazachos (2000) for the seismic hazard map of Greece and was used in the seismic hazard assessment developed by SEAHELLARC Working Group (2010). This zonation is quite large and only its western part was considered as we take into account SZs as far as 300 km from Pylos, at maximum. The only modification introduced in the Papaioannou and Papazachos (2000)

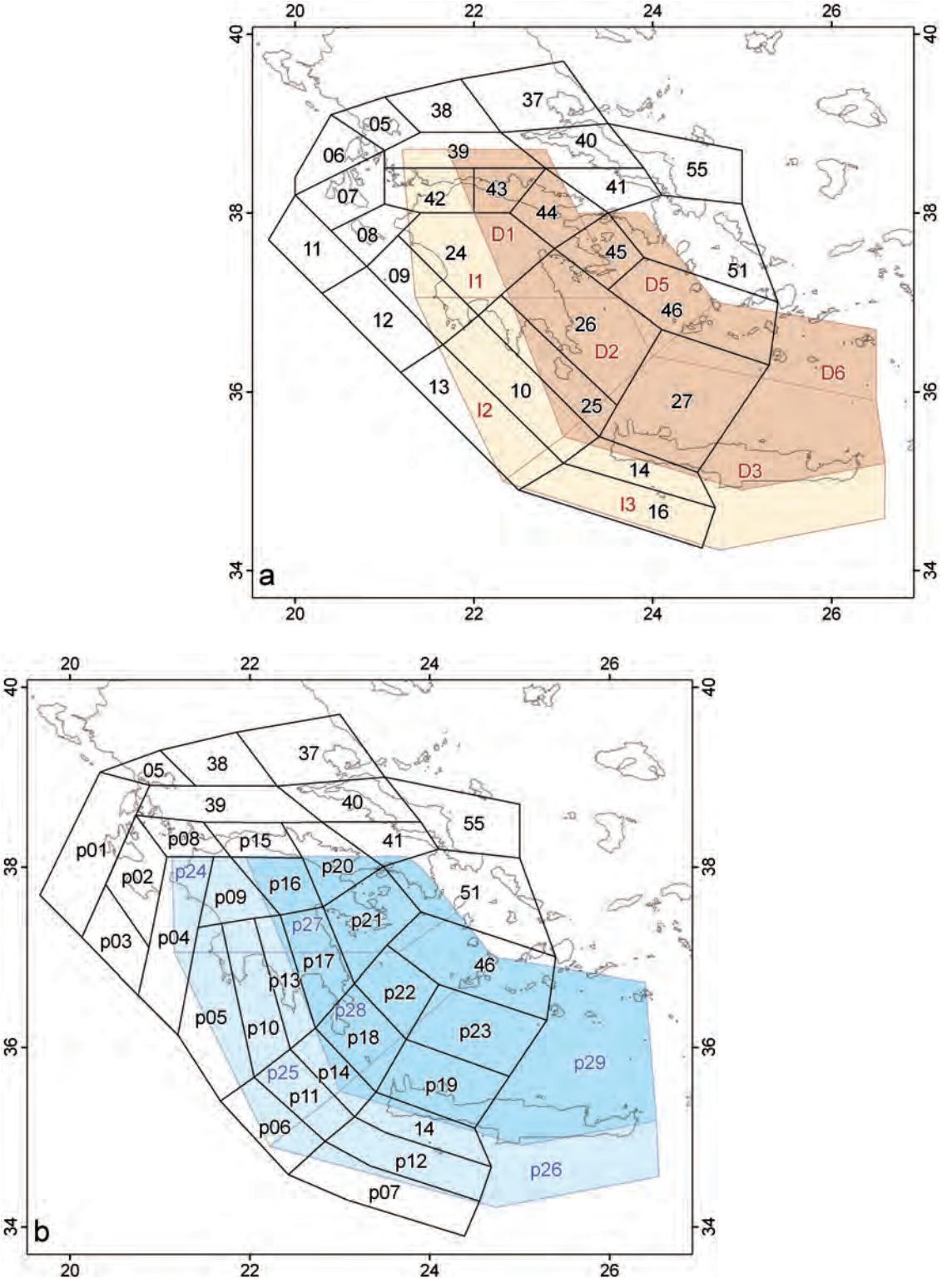

Fig. 4 - Seismogenic zonations used in the PSHA of the Pylos broader area: a) modified Papaioannou and Papazachos (2000) zonation; b) SEAHELLARC zonation (SEAHELLARC Working Group, 2014). The intermediate SZs are highlighted with a light colour and the deep SZs are marked with a dark colour.

zonation refers to the western limit of the SZs with an intermediate depth: it has been modified in agreement with the geometry of the subduction plane as proposed by Papazachos *et al*. (2000b), whose western limb is located offshore Peloponnese, and with the accepted evidence of a dip of about 35° for this subduction plane. Consequently, three intermediate SZs have been designed between 30 and 60 km depth, and three deep SZs from 60 to 100 km depth, and two very deep SZ from 100 km depth downwards, as far as 160 km (Fig. 4a). In summary, 35 SZs were used for hazard computation: 27 are shallow (modelled by a horizontal plane at the 15-km depth), 3 are intermediate, and 5 are deep. In addition, 3 large background zones have been considered. One collects the shallow events outside the actual shallow SZs, and it is modelled by a horizontal plane at the 15-km depth. The second takes the intermediate events external to the actual intermediate SZs and is modelled by a horizontal plane at the 45-km depth. The third has the deep events external to the actual deep SZs and is modelled by a horizontal plane at the 100-km depth.

The second zonation (Fig. 4b) has been defined in the frame of the SEAHELLARC project and it refers only to the Pylos broader area (see SEAHELLARC Working Group, 2014), while the rest was taken from the Papaioannou and Papazachos (2000) zonation with proper adjustments (Fig. 4b). More precisely, all the SZs along the coast have been reshaped, introducing the geometry of some SZs where dextral strike-slip faults and thrusting dominate. Entering into details, two SZs with transcurrent character have been introduced: the Cephalonia (p01) and the Andravida SZs (p04). Both these zones are typical for crustal seismicity and are deforming by dextral strike-slip. They are separated by two zones with thrust character (p02 and p03). The general shape of the Hellenic Arc appears in the Pylos area, with SZs p05, p10, and p13, that are linked eastwards with the original SZs of Papaioannou and Papazachos (2000). In these zones we can distinguish two levels of deformation: the shallow one, within the upper crust, is associated with thrusting of the Alpine units to the west, whereas the deeper seismicity, mainly linked with the subducted oceanic slab below continental Greece, shows compression and strike-slip movement. Minor changes have also been introduced to several SZs on mainland. The intermediate and deep SZs of Papaioannou and Papazachos (2000) have been also modified to shape with continuity the dipping plane between 30 and 60 km, in agreement with the modification described before for the Papaioannou and Papazachos (2000) zonation, and have been subdivided as cited before. The same large background zones, as those described for the previous zonation have been considered as well.

3.2. Seismicity parameters

The seismicity parameters used for seismic hazard assessment by the CRISIS code (Ordaz *et al*., 2007) are the *a*- and *b*-values of the Gutenberg - Richter (GR) relation and M_{max}. The description of the seismicity parameters for the part of the logic tree referring to the P&P zonation has been already presented in details in the second step of the seismic hazard assessment of SEAHELLARC Working Group (2010), only those for the PYL zonation are, consequently, described here.

Individual seismicity rates have been computed following two different approaches: the "higher not highest" (HNH) method and the Albarello and Mucciarelli (2002: A&M) method; both approaches were already applied for the seismic hazard maps of the Italian territory (Slejko *et al*., 1998; Albarello *et al*., 2000) and take into account in different ways the completeness of the earthquake catalogue. As in the preliminary elaborations (SEAHELLARC Working Group,

2010), the maximum likelihood method (MLM) has been applied for assessing the *a*- and *b*-values of the GR relation. The seismicity parameters are reported in Table 2 together with the value of the minimum magnitude (M_{min}) considered in the regression analysis.

M_{max} was estimated according to two different approaches: the first is statistical and based on the earthquake catalogue contents (K&G: Kijko and Graham, 1998) while the second is based on the available geological information (GEO: Wells and Coppersmith, 1994).

3.2.1. The statistical M_{max}

The K&G approach requests the values of the maximum observed magnitude, the seismicity parameters, and the completeness interval of the catalogue used for the assessment of the parameters. For the HNH approach for seismicity rate computation, the completeness period of the maximum observed magnitude (M_{obs}) in the SZ was taken as catalogue completeness, because the individual magnitude rates are normalized on the basis of their most active period. For the A&M approach, the period of the last 300 years has been considered arbitrarily as complete, because the method weights the rates of different time intervals according to the probability that they are complete and this period is long enough to avoid much larger M_{max} values considering longer periods. The computed values of M_{max} are reported in Table 2, with reference to the SZs of the PYL zonation. It was possible to compute an M_{max} different from M_{obs} almost for all SZs and the increment computed with respect to M_{obs} is, in a few cases, rather large: this depending on the short completeness period considered.

3.2.2. The geological M_{max}

The second method for M_{max} computation (GEO) is a geological approach and it is based on the tectonic characteristics of each SZ. This approach was applied only for the PYL zonation, where the SZs have a well defined seismotectonic character. More precisely, the main tectonic feature was identified in each SZ and its length was estimated.

The GEO approach for the determination of M_{max} for a seismogenic source is based on the scaling law between surface rupture length (*SRL*) and maximum (or characteristic) magnitude established by Wells and Coppersmith (1994) for earthquakes in California. Pavlides and Caputo (2004) developed a similar relation also for earthquakes in Greece. The concept of characteristic earthquake was introduced by Schwartz and Coppersmith (1984) and states that each fault produces only earthquakes of a well defined magnitude (with a 0.3 range of uncertainty): i.e., the characteristic magnitude of that fault. Without entering into the debate if this statement holds for all faults or only for some specific ones, it is reasonably to accept a maximum possible rupture length for each fault and, consequently, to derive its maximum possible magnitude. A further simplification is here introduced considering as identical *SRL* and fault rupture length.

The Wells and Coppersmith (1994) relation for an average focal mechanism was established on 77 events in the M_W range 5.2 to 8.1 and has the form:

$$M_W = 1.16 \log SRL + 5.08. \quad (5)$$

The Pavlides and Caputo (2004) relation was established on 36 events in the M_S range 5.2 to 7.5 that occurred in Greece and has the form:

Table 2 - Statistical M_{max} for the PYL zonation. T is the completeness period considered, M_{min} is the minimum magnitude considered in the regression, a and b are the parameters of the GR relation. A 2000-year period was used in the A&M approach for SZ p12 because of the long span of the SZ catalogue, very large standard deviations (SDs) obtained with shorter periods, and agreement with the period of the HNH approach.

SZ	M_{obs}	HNH						A&M					
		T	M_{max}	SD	M_{min}	a	b	T	M_{max}	SD	M_{min}	a	b
005	6.2	159	6.2	0.22	3.7	4.58	1.06	300	6.2	0.21	3.7	4.64	1.10
014	7.2	259	7.4	0.22	3.7	5.04	1.05	300	7.7	0.46	4.3	6.98	1.31
037	7.0	259	7.1	0.22	3.7	4.40	0.93	300	7.3	0.36	3.7	5.47	1.27
038	6.5	109	6.7	0.33	3.7	6.26	1.41	300	6.6	0.32	3.7	7.16	1.66
039	7.0	259	7.1	0.22	3.7	5.29	1.09	300	7.2	0.28	3.7	5.79	1.27
040	7.2	259	7.4	0.24	3.4	4.46	0.94	300	7.6	0.33	3.4	4.82	1.10
041	6.5	109	6.5	0.22	2.8	3.65	0.82	300	6.5	0.22	3.1	4.10	0.99
046	6.5	109	6.6	0.27	3.4	3.44	1.08	300	7.0	0.43	3.4	3.76	1.36
051	6.4	109	6.6	0.26	2.8	3.48	0.84	300	6.7	0.40	3.1	4.52	1.23
055	5.9	99	5.9	0.22	3.4	4.88	1.13	300	5.9	0.20	3.4	4.95	1.16
p01	7.4	259	7.4	0.21	3.7	4.91	0.92	300	7.4	0.21	3.7	4.74	0.91
p02	7.2	259	7.4	0.21	3.7	4.79	0.93	300	7.4	0.22	3.7	5.13	1.04
p03	6.8	59	6.8	0.25	3.4	4.48	0.90	300	6.8	0.21	3.4	4.49	0.94
p04	7.0	259	7.0	0.21	3.7	5.65	1.12	300	7.1	0.22	3.7	5.92	1.21
p05	7.5	409	7.8	0.26	4.0	5.72	1.15	300	7.9	0.36	4.0	6.05	1.25
p06	6.0	109	6.4	0.34	4.3	5.99	1.39	300	6.3	0.26	4.3	6.14	1.44
p07	6.4	109	6.6	0.28	3.7	4.05	0.92	300	6.5	0.21	3.7	3.42	0.80
p08	6.4	109	6.6	0.27	3.7	4.49	1.03	300	6.6	0.27	3.7	5.65	1.35
p09	6.4	109	6.6	0.28	3.7	6.09	1.35	300	6.7	0.32	3.7	6.90	1.62
p10	6.8	159	6.8	0.23	3.7	5.50	1.09	300	6.8	0.25	3.7	6.28	1.22
p11	6.2	109	6.3	0.25	4.0	5.35	1.20	300	6.2	0.22	4.0	5.65	1.29
p12	8.3	2009	8.3	0.21	3.7	4.51	0.94	2000	8.5	0.36	4.3	5.58	1.20
p13	6.8	159	6.9	0.28	3.4	4.40	1.09	300	7.0	0.39	3.4	5.83	1.22
p14	7.0	259	7.4	0.39	3.7	5.04	1.05	300	7.7	0.46	3.7	5.96	1.31
p15	6.8	259	6.8	0.21	3.7	5.77	1.19	300	6.9	0.26	3.7	6.48	1.44
p16	6.8	159	6.8	0.23	3.4	4.11	0.92	300	6.9	0.28	3.4	4.92	1.18
p17	6.1	109	6.2	0.21	3.4	5.39	1.09	300	6.2	0.25	3.4	5.85	1.22
p18	7.2	100	7.6	0.32	3.7	6.46	1.36	300	7.9	0.65	3.7	6.42	1.53
p19	6.0	109	6.3	0.31	4.0	8.48	1.36	300	6.3	0.26	4.3	6.48	1.53
p20	6.8	159	6.8	0.21	3.1	3.96	0.85	300	6.8	0.22	3.1	4.14	0.97
p21	6.5	109	6.6	0.29	3.4	3.98	0.96	300	6.6	0.28	3.1	4.17	1.08
p22	5.3	99	6.9	0.28	3.7	6.25	1.08	300	7.0	0.33	3.7	6.75	1.36
p23	6.7	159	6.9	0.28	3.7	5.62	1.08	300	7.4	0.37	3.7	6.19	1.36
p24	5.0	32	5.0	0.22	3.7	5.94	1.45	300	5.0	0.20	3.7	8.12	1.52
p25	6.7	98	6.9	0.30	4.0	5.36	1.14	300	6.8	0.21	3.7	5.86	1.04
p26	6.6	98	6.8	0.25	4.3	6.43	1.27	300	6.8	0.21	4.0	6.61	1.13
p27	7.2	164	7.4	0.25	3.4	3.60	0.79	300	7.4	0.24	3.4	2.83	0.68
p28	7.2	164	7.5	0.31	3.7	3.88	0.86	300	7.4	0.24	3.7	3.35	0.59
p29	8.2	2009	8.2	0.20	4.3	3.73	0.70	300	8.3	0.21	4.3	3.87	0.67

$$M_S = 0.90 \log SRL + 5.48. \quad (6)$$

Interesting considerations about *SRL* and total fault length are proposed by Pavlides and Caputo (2004): they found that about 50% of the investigated earthquakes ruptured almost their entire fault length, while longer structures ruptured about the half of their total length. As both Eqs. (5) and (6) were calibrated for events with a magnitude larger than 5.2 and their application in our study region refers almost exclusively to events of magnitude 6 and above, we can consider M_S equivalent to M_W, according to the relations of Papazachos and Papazachou (1997) that we have applied to construct the SEAHELLARC earthquake catalogue.

When no surface evidence is available, there is no univocal definition about what the *SRL* should be intended and the general use is to take the half of the total fault length (Mark, 1977). We took the half of the total fault length as rupture length, when not explicitly declared (Pavlides and Caputo, 2004), obtaining an M_{max} that is smaller sometimes than M_{obs} (see Table 2).

The description of the main tectonic element present in each SZ is fully given in SEAHELLARC Working Group (2014). We considered both scaling laws of Wells and Coppersmith (1994) and Pavlides and Caputo (2004) and the results are reported in Table 3. The average formulae have been applied because they are better constrained than those for the individual fault types. We can see that the obtained estimates are quite similar with the two formulae and they are in general similar to M_{obs}. Only in the case of two SZs (p02 and p05) we have obtained, with both relations, estimates of M_{max} which are remarkably lower than M_{obs}, while M_{max} is only slightly lower than the observed value in SZ p01. Conversely, the M_{max} estimates for SZ p17 are remarkably higher than M_{obs}.

In conclusion, considering the similarities of the estimates obtained with the two relations, we decided to prefer the Pavlides and Caputo (2004) one because it was calibrated specifically on Greek earthquakes; obviously, when M_{obs} is larger than M_{max} the former is taken as M_{max}.

Table 3 - M_{max} values obtained using the Pavlides and Caputo (2004) (M_{PC}) and the Wells and Coppersmith (1994) (M_{WC}) formulae considering the half of the total length (L) as rupture length. M_{obs} is the maximum observed magnitude. All magnitudes are M_W.

SZ	L(km)	M_{obs}	M_{PC}	M_{WC}
p01	153.5	7.4	7.2	7.3
p02	66.3	7.3	6.9	6.8
p03	45.7	6.6	6.7	6.7
p04	136.0	7.0	7.1	7.2
p05	110.9	7.5	7.1	7.1
p09	40.3	6.4	6.7	6.6
p10	70.3	6.7	6.9	6.9
p13	110.1	6.8	7.1	7.1
p15	60.7	6.8	6.8	6.8
p16	66.5	6.8	6.9	6.9
p17	91.6	6.1	7.0	7.0
p20	63.5	6.8	6.8	6.8
P21	58.9	6.7	6.8	6.8

3.4. Ground motion prediction equations

The most popular European GMPE [Ambraseys *et al*. (1996: AMB)] and one of the most recent Greek ones [Skarlatoudis *et al*. (2003: SKA)] have been considered in the present study for shallow earthquakes. As the contribution of intermediate and deep earthquakes could be important, two further GMPEs for subduction zones around the world [Atkinson and Boore (2003: A&B) and Youngs *et al*. (1997: YOU)] have been considered for the events with a focal depth larger than 30 km.

For a correct application of these GMPEs, the intermediate and deep SZs have been subdivided in narrow slices. In fact, the computer code CRISIS (Ordaz *et al*., 2007), chosen for the seismic hazard assessment in the SEAHELLARC project, uses a table of ground motion vs. epicentral or hypocentral distance to compute the ground shaking at the site according to the site to source distance. The table, then, cannot take into account different depth values of a dipping plane. Both Youngs *et al*. (1997) and Atkinson and Boore (2003) attenuation relations for deep earthquakes (subduction zones and in slab events, respectively) use the Joiner and Boore (1981) distance (equivalent to the epicentral distance in our case) and have a term directly dependent on the depth value. This depth-depending term multiplies by $e^{0.00607h}$ and $10^{0.0113h}$, respectively, the *PGA* value and, consequently, it produces a difference respectively of about 6% and 30% changing the depth by 10 km. Consequently, the GMPEs can be applied only in an approximated way in the case of deep SZs, by considering small SZs with variable depth not greater than 20 km and by constructing the attenuation table for the mean depth of these small zones. For a correct application of the GMPEs, the intermediate and deep SZs have been subdivided into 15-km and 20-km thick slices for intermediate and deep SZ, respectively, to avoid too rough approximations. This limitation of the CRISIS code that we have applied was eliminated in the last version of the same code (Ordaz *et al*., 2012) that was not available at the time of our processing.

Moreover, it is important to pay attention to the magnitude, distance, and depth ranges of the GMPEs. Considering the intraslab (in-slab) formulation, the distance range of application is 30-350 km and the magnitude range is 5.0-7.5 for both GMPEs. The Atkinson and Boore (2003) GMPE fixes the depth at 100 km for greater depths.

The shallow GMPEs are defined for distance from the fault, while the non-shallow GMPEs are defined for hypocentral distance: the related options have been considered in the CRISIS code.

All GMPEs were defined for M_W and the related magnitude ranges and standard deviations are reported in Table 4. All the GMPEs were extrapolated outside their range (Ambraseys, 1995) as seismicity rates of magnitude classes below 4.5 were also used in the hazard computation. Fig. 5 shows the behaviour of these four GMPEs.

Table 4 - GMPEs used in the hazard computation. The Youngs *et al*. (1997) GMPE is defined only for rock and soil: we have associated the soil version to both stiff and soft soil σ_a is the standard deviation.

GMPE	Soil	M_W Range	σ_a	Type
Ambraseys *et al.* (1996)	Rock, stiff, soft	4.9-7.5	0.576	shallow
Skardatoulis *et al.* (2003)	Rock, stiff, soft	4.5-7.0	0.658	shallow
Atkinson and Boore (2003)	Rock, stiff, soft	5.0-8.3	0.622	int. & deep
Youngs *et al.* (1997)	Rock, soil	5.0-8.2	0.850	Int. & deep

3.5. Seismic hazard maps for the Pylos broader area

Twenty-four branches constitute the logic tree (Fig. 3): 2 zonations, 2 methods to compute seismicity rates, 2 maximum magnitude estimates [only 1 for the Papaioannou and Papazachos (2000) zonation], and 4 GMPEs. The aleatory uncertainties of the GMPEs have been taken into account by introducing their standard deviation (σ_a) into the computation.

A total of 72 runs of the CRISIS code (Ordaz *et al*., 2007) have been processed in order to compute the hazard results of all the branches of the logic tree for each of the 3 soil types: rock, stiff, and soft soil (Figs. 6 to 8). All these maps show the mean [see discussion about mean and median hazard estimates in Abrahamson and Bommer (2005), McGuire (2005) and Musson (2005)] *PGA* with a return period of 475 years calculated by weighted interpolation of the branch probabilities.

Fig. 9 represents the final results, showing the *PGA* which is the mean value of the 24 hazard curves from which the maps of Figs. 6 to 8 were constructed (the dispersion of the hazard curves σ_e is not added in these maps) respectively for rock (Fig. 9a), stiff soil (Fig. 9c), and soft soil (Fig. 9e). These maps can be compared with the usual hazard maps that were computed before the introduction of the logic tree approach. In order to quantify the overall uncertainty of the results, we computed the coefficient of variation (*COV*: Cramer *et al*., 2002), which is the standard deviation (σ) of the estimated *PGA* variation at each point divided by the mean value at that point ($COV=\sigma/PGA_{\text{mean}}$). It can be seen from all Figs. 9b, 9d, and 9f that the *COV* value remains below 30% almost everywhere. This means that there is not a large uncertainty associated to the estimates here represented. The largest uncertainties are found in the north-easternmost corner of the study region, well far away from the Pylos area, where the *COV* value is below 18%. It is clear that a logic tree with a larger number of branches, i.e., with more options for the input parameters, would have implied a larger epistemic uncertainty on the mean results, but at the present stage we do not see any need to implement the logic tree with additional options.

The influence of the individual input parameters in the final hazard results is smoothed by the use of several different hypotheses (branches). To explore this aspect, i.e., to determine individual branch-point sensitivity, we computed the individual coefficient of variation (*ICOV*) for each alternative (node) of the logic tree (zonation models, seismicity models, M_{max}, and GMPEs). Each *ICOV* map represents the relative contribution of the uncertainty in that variable to the overall uncertainty presented in the *COV* map, while all the other variables remain fixed (Fig. 10). It can be seen that the major contribution to the overall uncertainty comes from the seismicity models, while M_{max} plays almost no influence for the 475-year return period. Only the results for rock are here presented as those for stiff and soft soil are similar.

In addition and according to the SSHAC (1997), estimates that take explicitly into account also the epistemic uncertainty (σ_e, scatter of the individual hazard curves, each calculated considering the aleatory variability) have been computed by adding one σ_e to the median *PGA*. Both estimates that add or not the epistemic uncertainty to the mean values, by the way, consider the epistemic uncertainties because they represent average values of the hazard curves coming from the several branches. Only the map accounting for the epistemic uncertainty referring to rock conditions is here reported (Fig. 11) and it shows again that the largest *PGA* (between 0.80 and 0.88 g) is expected in the Cephalonia and Zakynthos islands. The town of Pylos is characterized by ground motion values between 0.56 and 0.64 g. We can say, in general, that the explicit introduction of the epistemic uncertainty increases slightly more than 0.08 g the mean values of Fig. 9a.

For general purposes, a map showing the actual expected ground motion on the surface is of

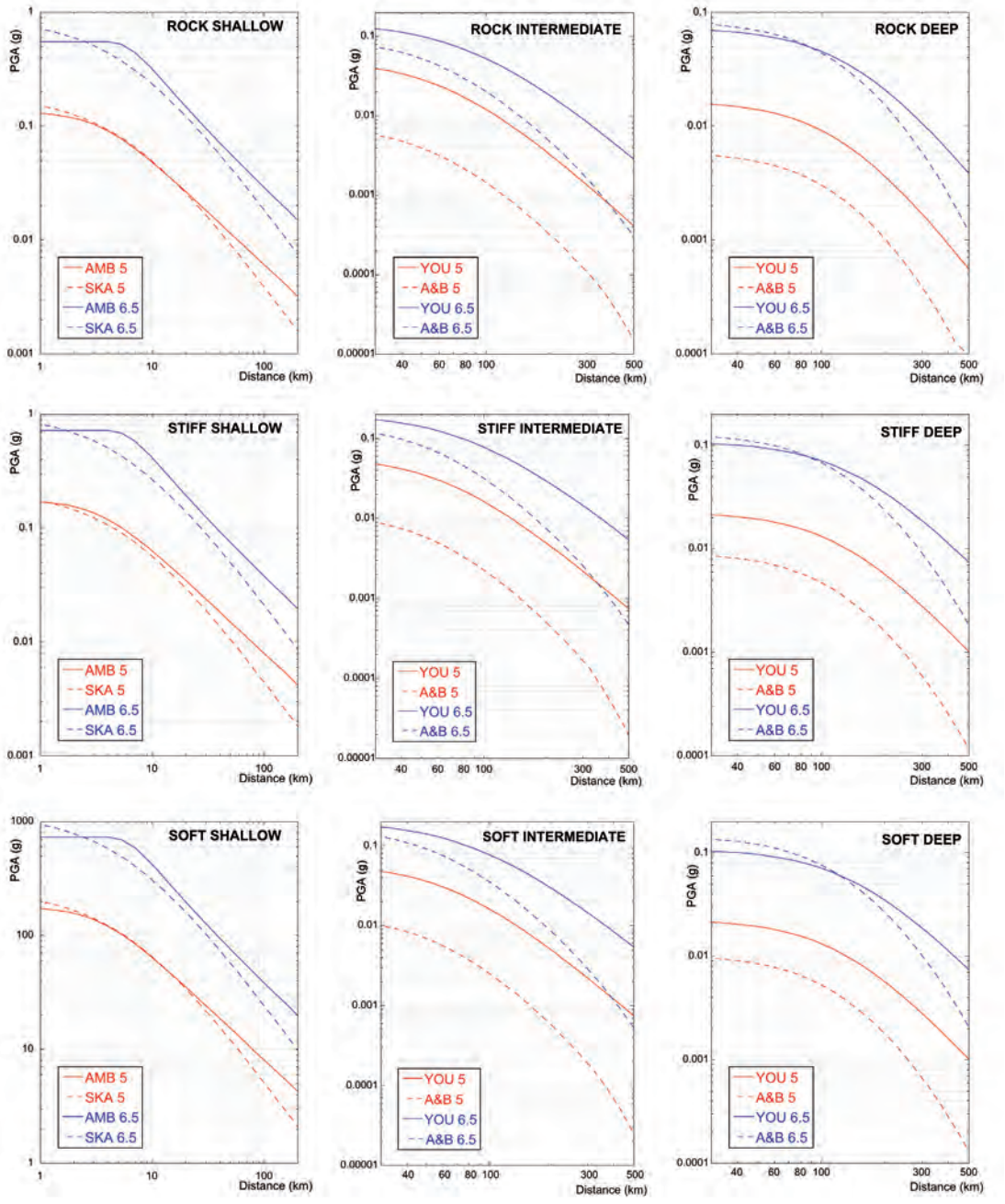

Fig. 5 - GMPEs used in the PSHA of the Pylos broader area for shallow, intermediate, and deep events (from left to right): first row) rock; central row) stiff soil; third row) soft soil.

paramount importance. For this reason, the specific soil conditions in a restricted territory around Pylos have been derived and the specific ground shakings (already shown in separate maps in Fig. 9) have been assembled by GIS facilities. Fig. 12a shows the soil types identified around Pylos (IGME, 1980): rock dominates and a large portion of the northern coastline of the gulf is characterized by stiff soil, while soft soil can be found only in limited spots along the northern coast. The seismic hazard map obtained by merging the results of Fig. 9 (Fig. 12b) displays that the largest

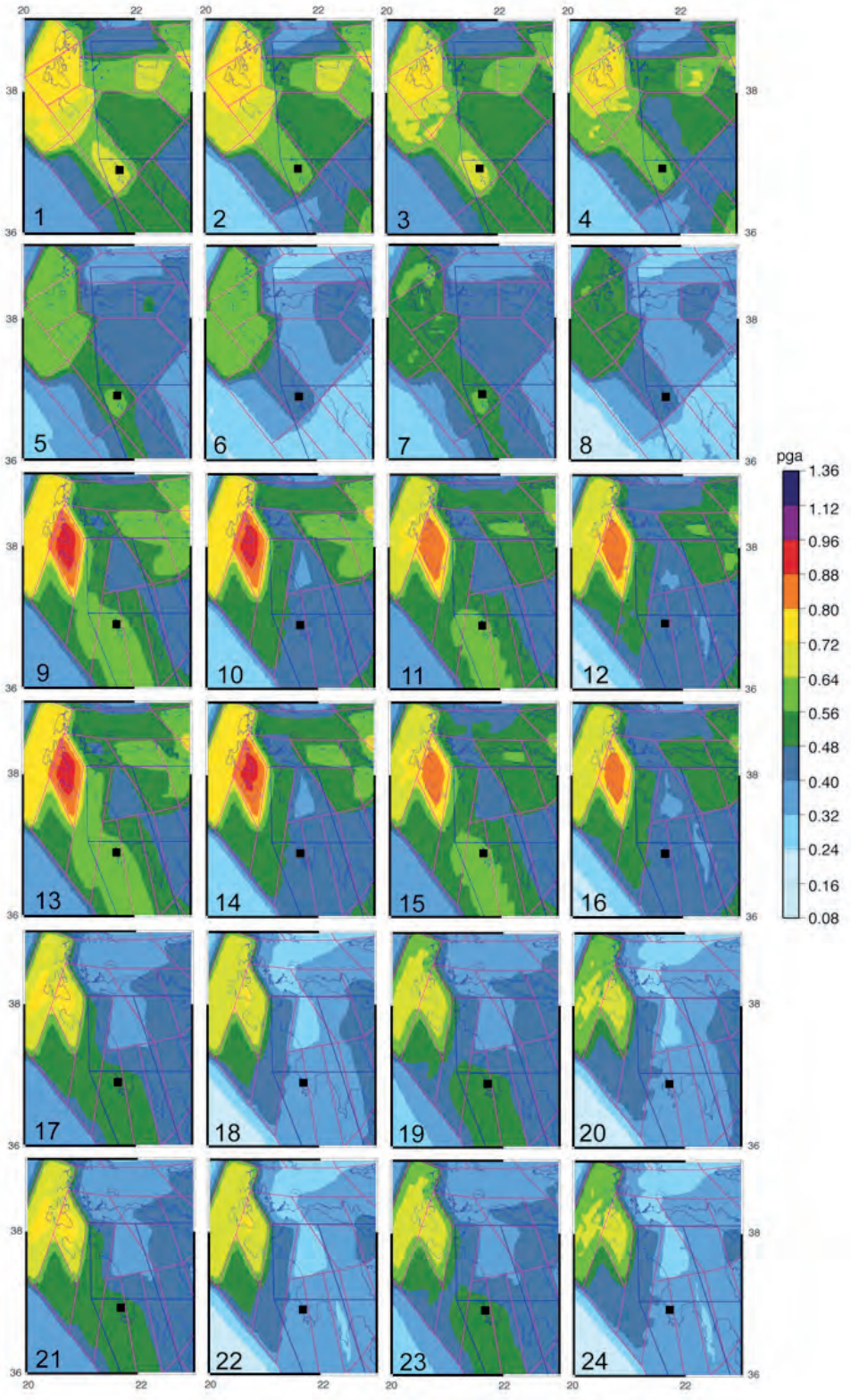

Fig. 6 - *PGA* with a 475-year return period in the Pylos broader area for rock conditions (results of the individual branches).

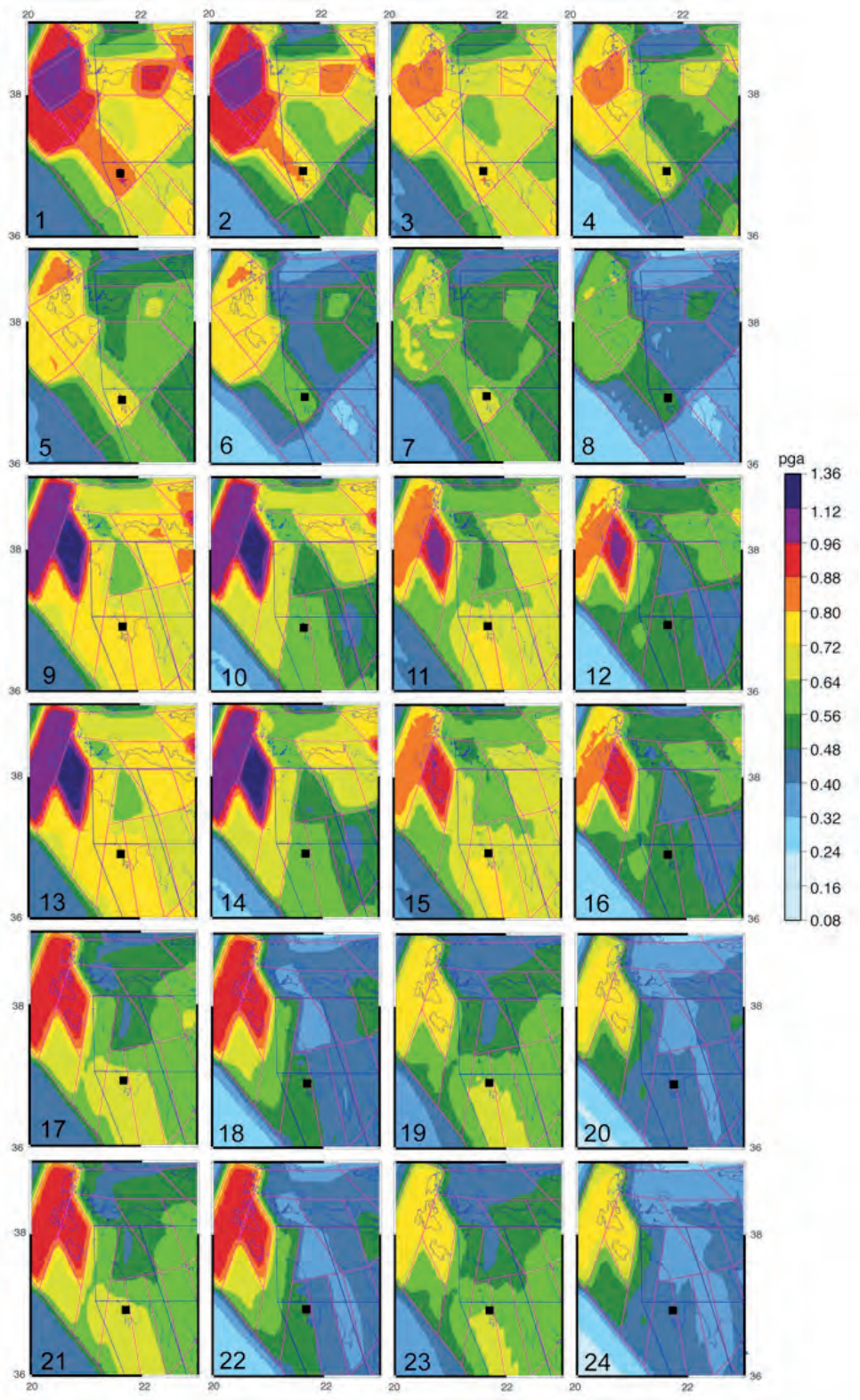

Fig. 7 - *PGA* with a 475-year return period in the Pylos broader area for stiff soil conditions (results of the individual branches).

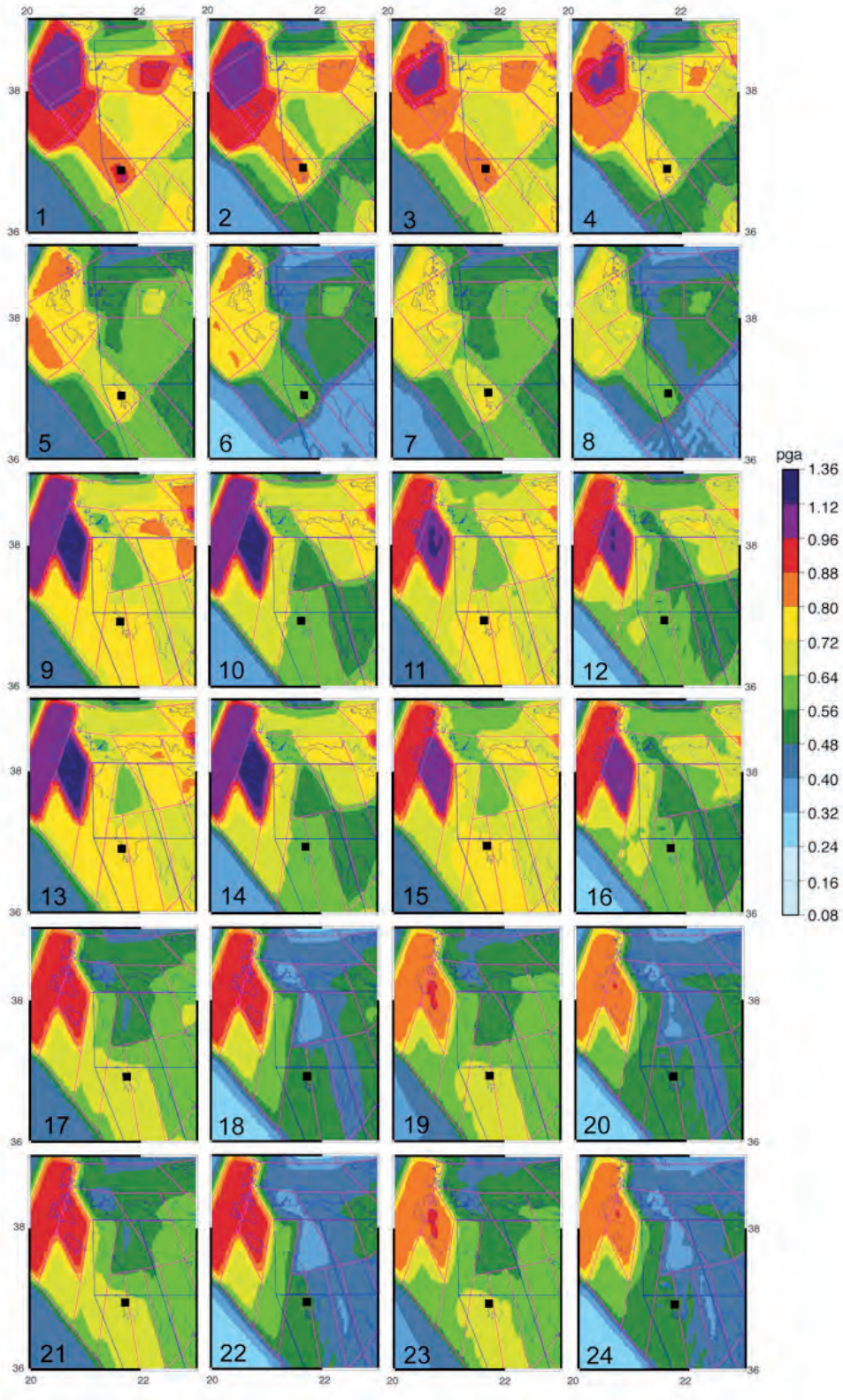

Fig. 8 - *PGA* with a 475-year return period in the Pylos broader area for soft soil conditions (results of the individual branches).

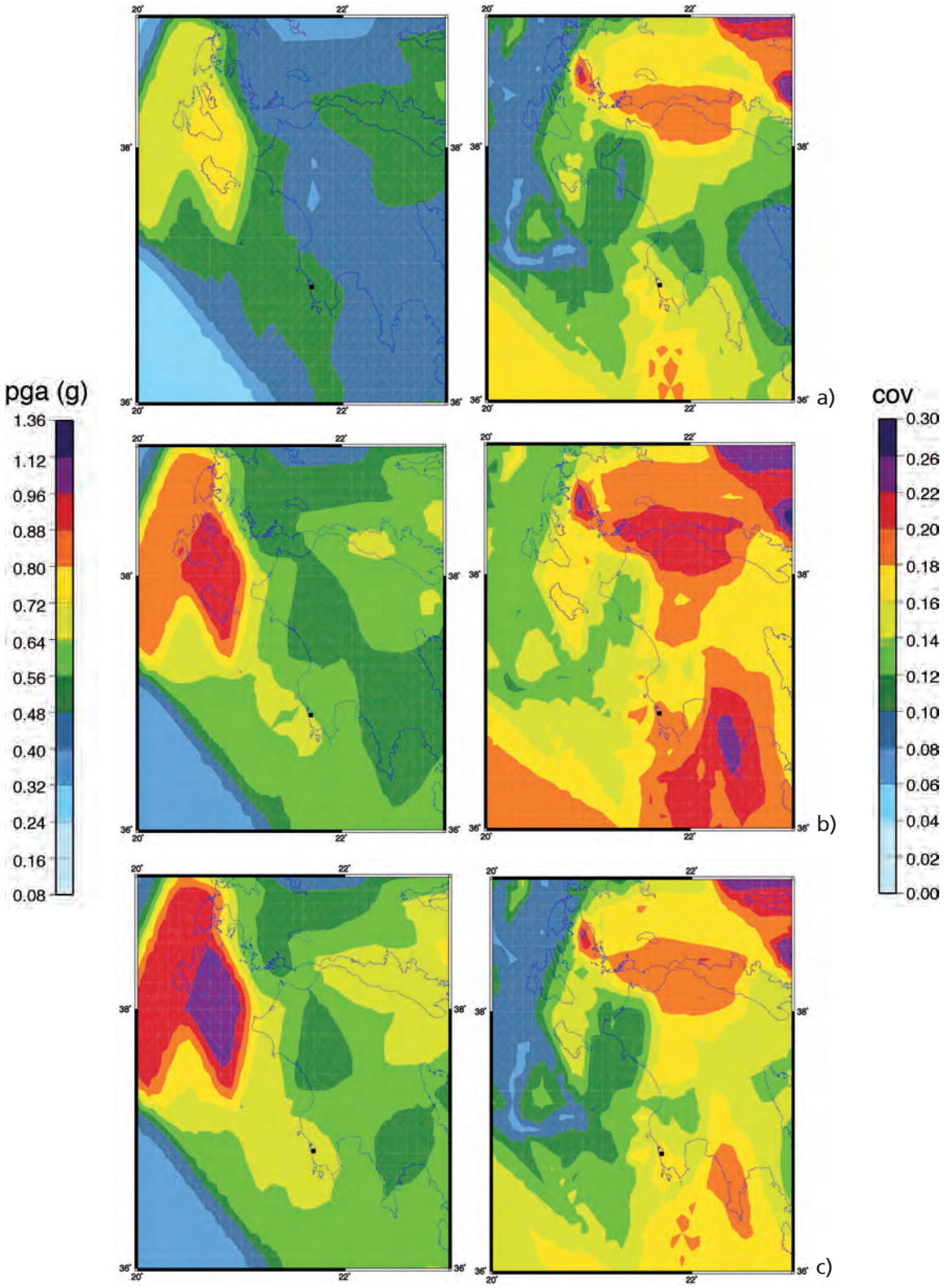

Fig. 9 - Mean *PGA* with a 475-year return period in the Pylos broader area (left) and related *COV* (right) for different soil conditions: a) rock; b) stiff soil; c) soft soil.

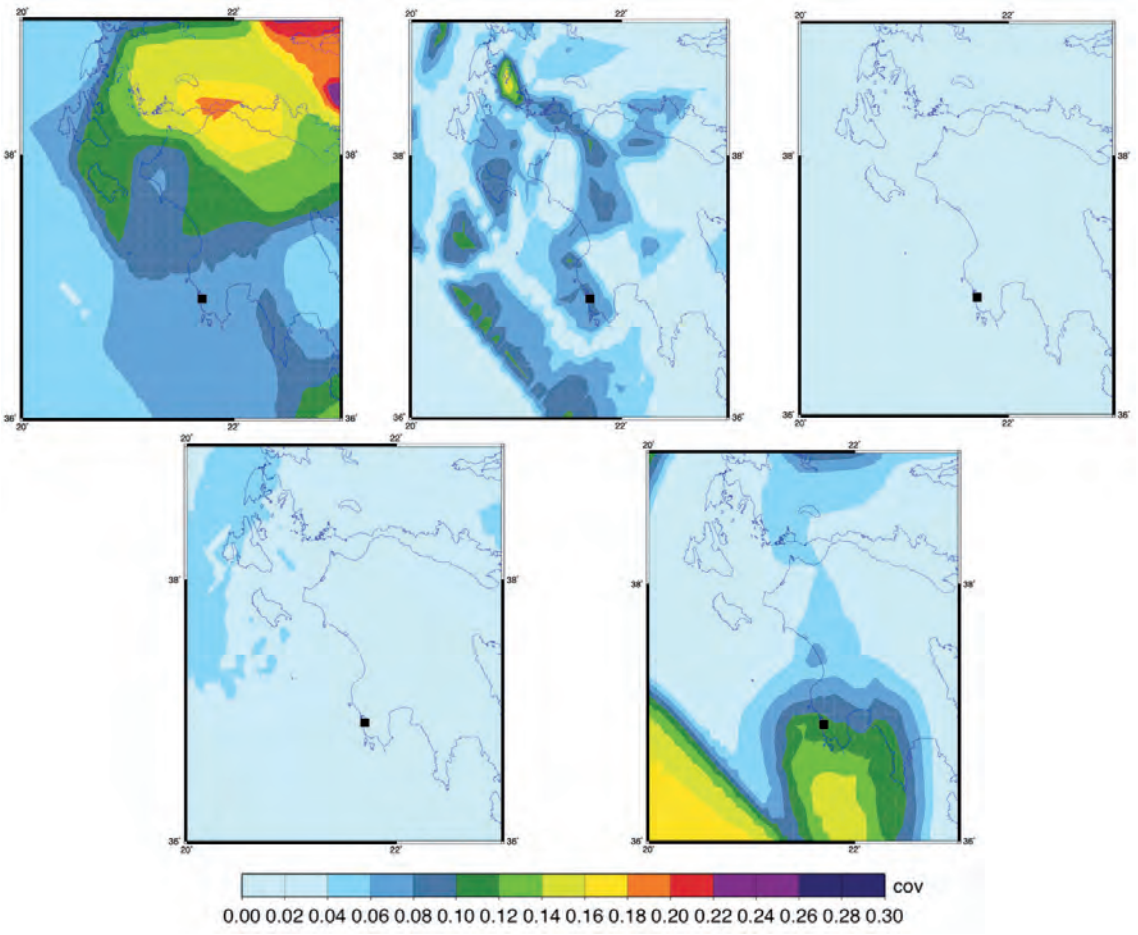

Fig. 10 - *ICOV* maps, related to *PGA* with a 475-year return period, in the Pylos broader area and rock conditions. From left top to right bottom: seismogenic zonation, seismicity rates, M_{max}, shallow GMPEs, intermediate and deep GMPEs.

ground motions are expected on soft (*PGA* larger than 0.650 g) and stiff (*PGA* between 0.625 and 0.650 g) soils, while values between 0.525 and 0.550 g are expected for the town of Pylos.

3.6. Seismic hazard in Pylos town

Concentrating the attention to the specific seismic hazard of Pylos, Fig. 13 shows the complete hazard curves for that site for the three soil categories, rock, stiff, and soft soil. In addition to the mean hazard curve (σ_a is always considered in the elaborations), also that increased by one σ_e is reported. The expected ground motion in Pylos (mean value of the 24 properly weighted branches of the logic tree) with a 475-year return period is 0.55 g (0.63 g if we add one σ_e) for rock sites, 0.72 g (0.85 g with one σ_e) for stiff soil sites, and 0.76 g (0.88 g with one σ_e) for soft soil sites. To point out the influence of the intermediate and deep SZs, an additional run has been done eliminating these zones from the zonation considered. We have obtained an expected shaking of 0.45 g (0.52 g with one σ_e) on rock. It means that the contribution of the intermediate and deep SZs is less than 10%, for the standard return period of 475 years.

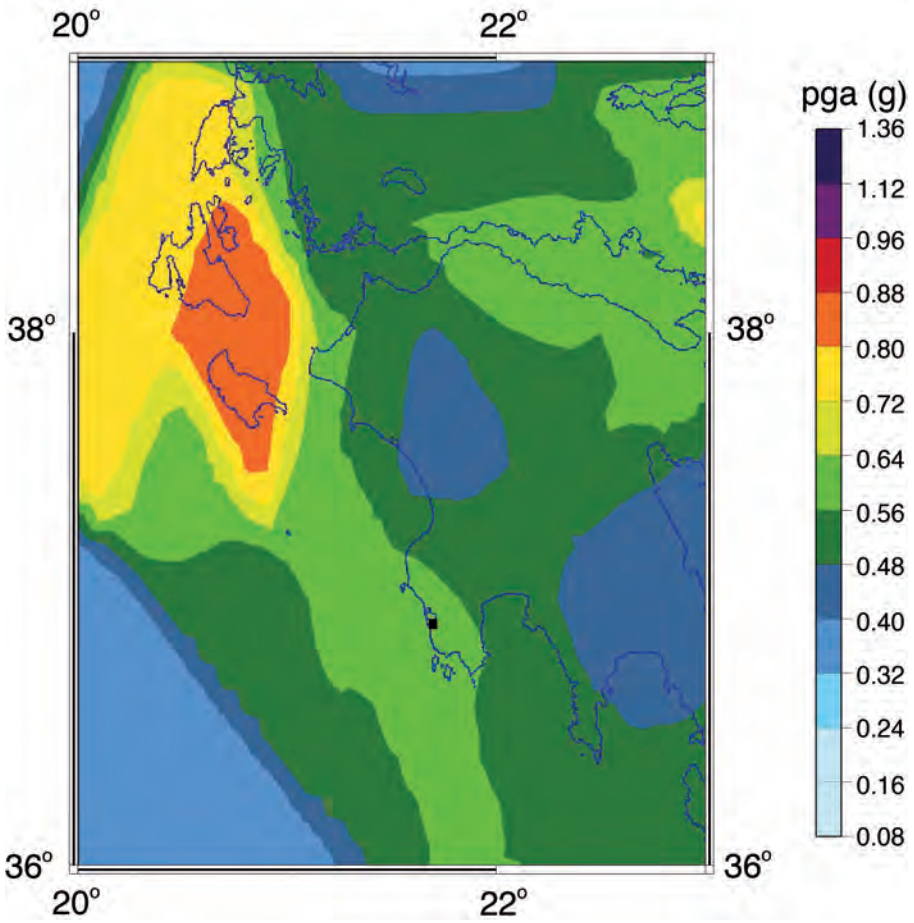

Fig. 11 - *PGA* with a 475-year return period in the Pylos broader area for rock conditions taking into account the epistemic uncertainty (see the text for the explanation).

3.7. Uniform hazard response spectra for selected sites

The uniform hazard response spectra (UHRSs) at 5% damping have been computed for the two sites of Pylos and Zakynthos using the same input as that used for *PGA*, with the exception of the elimination of the SKA GMPE because it is not defined for spectral ordinates but only for *PGA*. This fact does not represent a strong limitation of our analysis because the AMB GMPE is quite similar to the SKA one as it can be seen in Fig. 5.

As the AMB, A&B, and YOU GMPEs are defined for different periods, we have identified the 5 values that are present in all GMPEs, they are: 0.1 s, 0.2 s, 0.4 s, 1.0 s, and 2.0 s. The UHRS is, consequently, rather rough because it is based on 5 spectral ordinates only.

Fig. 14 shows the UHRS on rock for Pylos and Zakynthos. In addition to the mean value of the branches of the logic tree, the spectrum obtained adding one σ_e to the spectral coordinates is also shown. We have considered only the rock situation because Pylos town is geotechnically located on Pliocene formations (2.6-5.3 million years B.P.) such as marls and sandstones (IGME, 1980) and the city is surrounded by limestone hills of Paleocene-Eocene age (65-34 million years B.P.). As there are no boreholes or other geotechnical data available to support a quantification

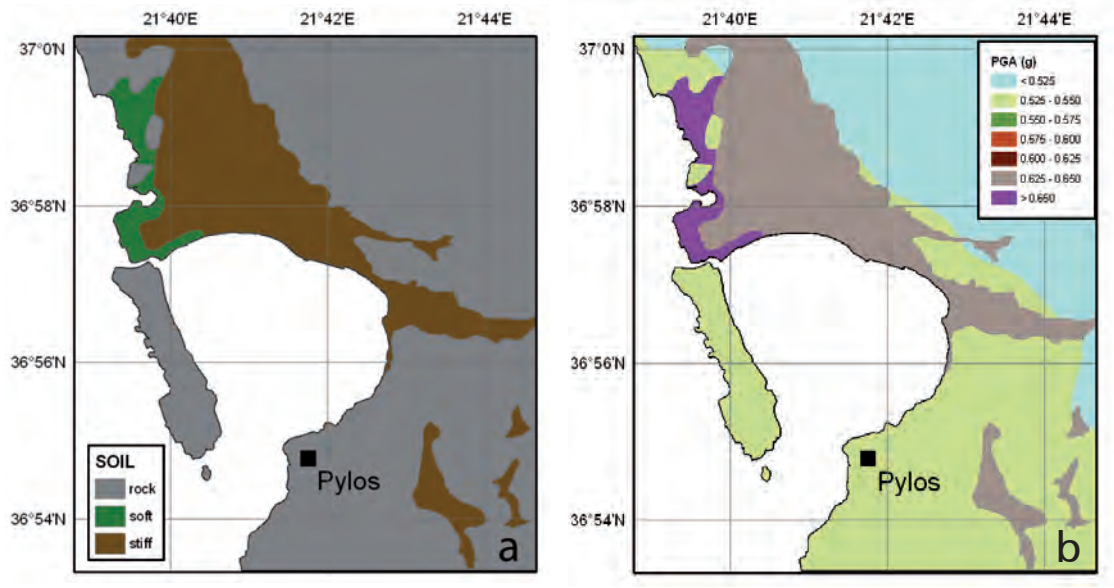

Fig. 12 - Soil seismic hazard for the Pylos area: a) soil map; b) *PGA* with a 475-year return period. Note that the classes from 0.550 to 0.625 g are not present.

of the shear wave velocities in these two formations, it seems reasonable to consider both these formations as rock [class A of the Eurocode 8 (CEN, 2002)]. In Zakynthos Island, rock conditions dominate as well.

3.8. Results for seismic risk assessment

Seismic risk assessment requires the convolution between the seismic hazard and the vulnerability curves. In Greece, as in most of the European countries, vulnerability curves have been defined in terms of macroseismic intensity as ground motion parameter, because of the scarcity of strong motion recordings. This fact implies that the computed *PGA* hazard curves are not suitable for risk assessment as they would require to be translated into intensity with the introduction of additional uncertainty. This translation resulted necessary to assess the estimated damage to buildings in Pylos (Pomonis and Gaspari, 2014).

One of the ground motion parameter which is considered well correlated with intensity is the Arias (1970) intensity (*Ia*). GMPEs for *Ia* have been recently provided for shallow earthquakes in Greece by Danciu and Tselentis (2007) for rock, stiff, and soft soil. Moreover, Tselentis and Danciu (2008) have established some scaling laws between *Ia* and macroseismic intensity: in addition to an average relation, these scaling laws have a term which takes into account the epicentral distance. GMPEs of *Ia* for deep earthquakes are very difficult to find. The only one we have been able to find refers to deep earthquakes in central America (Schmidt Diaz, 2008). Unfortunately, the standard deviation of this GMPE is not given but other statistical indicators of the quality of the fit (rather poor) are given. The Schmidt Diaz (2008) GMPE is defined for rock and soil, only. The same author defines a scaling law also between Modified Mercalli (MM) intensity and *Ia*: unfortunately also for this relation, no standard deviation is given.

We have considered the cited GMPEs and have introduced in the CRISIS code the GMPEs for *Ia*, arbitrarily assigning to the Schmidt Diaz (2008) GMPE the same standard deviation of

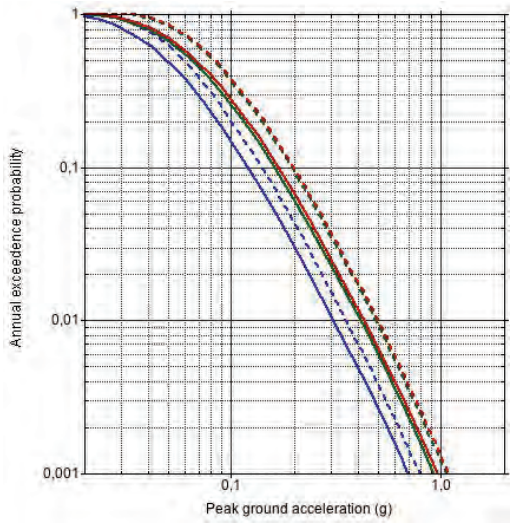

Fig. 13 - Seismic hazard curves for Pylos in terms of *PGA*: blue = rock, green = stiff soil, red = soft soil. Solid lines indicate mean values, dashed lines show mean values plus one σ_e. The curves for stiff and soft soils almost overlap.

the Danciu and Tselentis (2007) one. The seismic hazard curve for Pylos in terms of *Ia* has been obtained in such a way for the three soil types (Fig. 15). Moreover, the hazard curve in terms of *Ia* has been tentatively translated into MM intensity, without taking into account the uncertainty introduced in this transformation. Fig. 16 shows the seismic hazard curve for Pylos in terms of mean value in the MM intensity (no σ_e has been considered for the hazard curve in terms of *Ia*). It can be seen that, while the expected *PGA* for a 0.001 annual exceedence probability spans between 0.7 to 1.0 g, for rock and soft soil respectively (Fig. 13), the expected MM intensity is less than 7 for all soil types (Fig. 16a). This quite low intensity value [Tselentis and Danciu

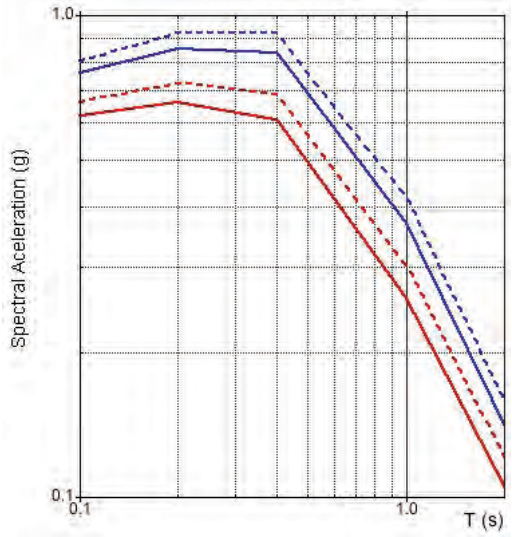

Fig. 14 - UHRSs on rock for a 475-year return period for Pylos (red lines) and Zakynthos (blue lines). Mean values are represented by solid lines and mean values plus one σ_e are represented by dashed lines.

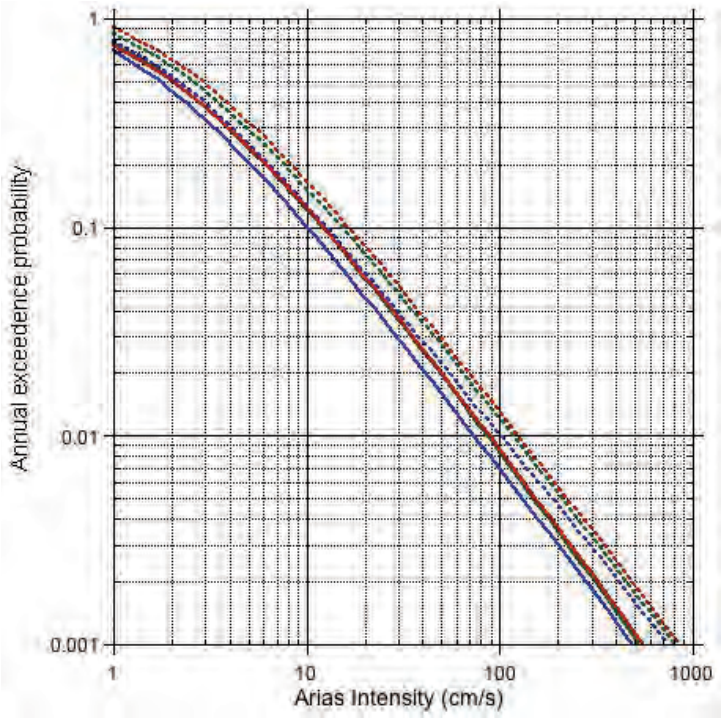

Fig. 15 - Seismic hazard curves for Pylos in terms of *Ia*: blue = rock, green = stiff soil, red = soft soil. Solid lines indicate mean values, dashed lines show mean values plus one σ_e. The mean curves for stiff and soft soils almost overlap.

(2008) associate a mean *PGA* value of 0.18 g to the MM intensity of 7] suggests that the applied *Ia* to MM intensity conversion is not satisfactory. We have, then, applied the Tselentis and Danciu (2008) mean scaling law, which does not consider the epicentral distance, also extrapolating it, when necessary. The obtained hazard curve (Fig. 16b) displays a value around intensity 10 for the annual exceedence probability of 0.001, which seems realistic and is suggested for seismic risk computation. In this case, the curves obtained by adding one standard deviation of the scaling law between *Ia* and MM intensity to the mean value is reported as well (see dashed lines in Fig. 16b).

4. Deaggregation of the seismic hazard results

It may be useful to estimate the seismogenic sources, sometimes even in terms of magnitude and distance pair, which contribute most to the hazard at the study site. This process is called deaggregation and is quite a new technique (Bazzurro and Cornell, 1999).

Fig. 17 shows the SZs of the PYL zonation used for the probabilistic seismic hazard assessment of Pylos and the major faults, considered for the estimation of the maximum magnitude (see SEAHELLARC Working Group, 2014). The SZs represented are only those that are close to Pylos and contribute more to hazard. As the aim of the SEAHELLARC project was seismic and tsunami risk reduction, we refer to the seismic hazard estimates related to the 475-year return period, standard feature in urban planning. Fig. 18 shows the result of the deaggregation: the

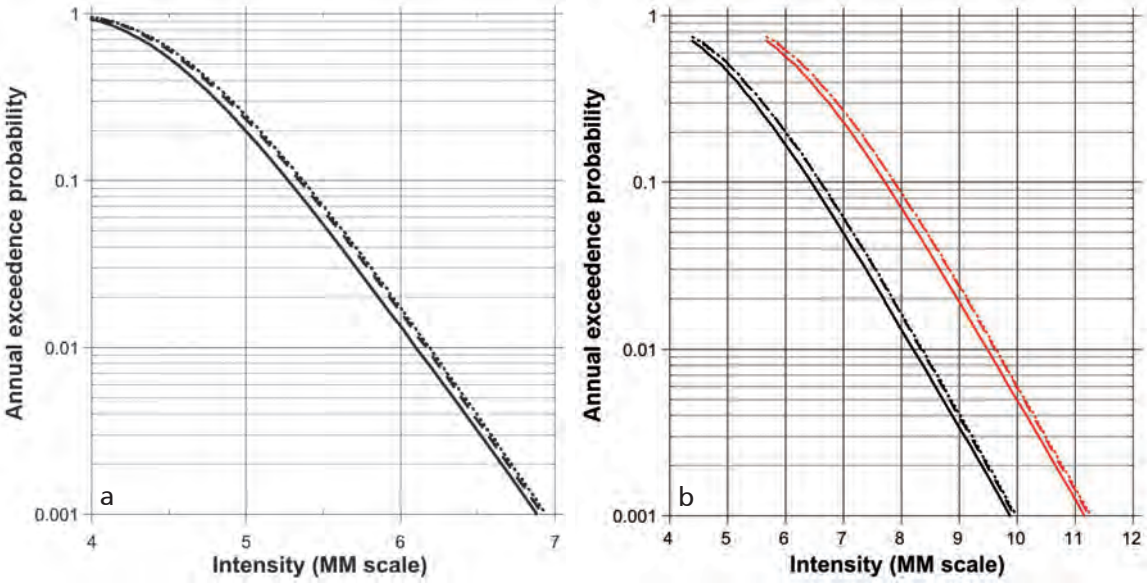

Fig. 16 - Seismic hazard curves for Pylos in terms of MM intensity: solid line = rock, dashed line = stiff soil, dotted line = soft soil. The curves for stiff and soft soils almost overlap. Tselentis and Danciu (2008) scaling law: a) considering the epicentral distance; b) without considering the epicentral distance, with (red) and without (black) standard deviation of the scaling law.

dominating SZs are p05, p10, p25i, and p04. The magnitude – distance deaggregation for SZ p25i has not been computed because it is an intermediate source, whose ground motion at the surface is conditioned by several factors and the main fault in the SZ has not been identified.

Once the potentially most dangerous SZs have been identified, the deaggregation in terms of distance and magnitude pairs has been performed by considering the lineament representing roughly the major fault identified inside each SZ (see SEAHELLARC Working Group, 2014). The results coming from the branch that most approaches those of the final mean value map (Fig. 9a) have been elaborated: in details, these results derive from the branch PYL, HNH, K&G, AMB, and A&B.

Figs. 19a to 19c show the results of the deaggregation for the most dangerous SZs for Pylos: p05, p10, and p04. It can be seen that the most contributing bin of the major fault inside SZ p04 is identified by a distance of 55 km from Pylos and a magnitude of 6.8. For SZ p05, the most contributing bin has a distance of 15 km and a magnitude of 6.9. The distance of 25 km and the magnitude of 6.5 identify the bin that contributes mostly in SZ p10. It is worth noting that the cited magnitudes come from the deaggregation analysis and do not correspond generally to the maximum possible event for the SZ (they are some magnitude units lower).

As the largest earthquakes, and several strong tsunamis, in the Ionian Sea were generated in the Cephalonia region, an additional investigation has been done for the SZs of the Ionian islands of Cephalonia and Zakynthos (SZs p01, p02, and p03 in Fig. 17a). The results are reported in Figs. 19d to 19f. It can be seen that the most contributing bin of the major fault inside SZ p01 is identified by a distance of 180 km from Pylos and a magnitude of 7.4. For SZ p02, the most contributing bin has a distance of 90 km and a magnitude of 6.8. This result has been obtained by excluding the maximum event (the 1953 earthquake with an M_W of 7.3) which occurred in

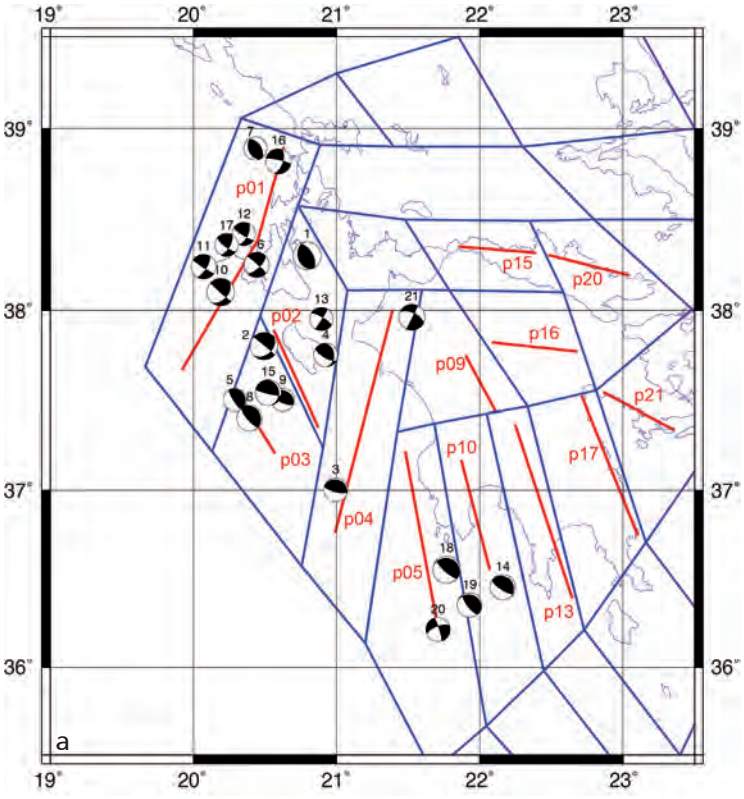

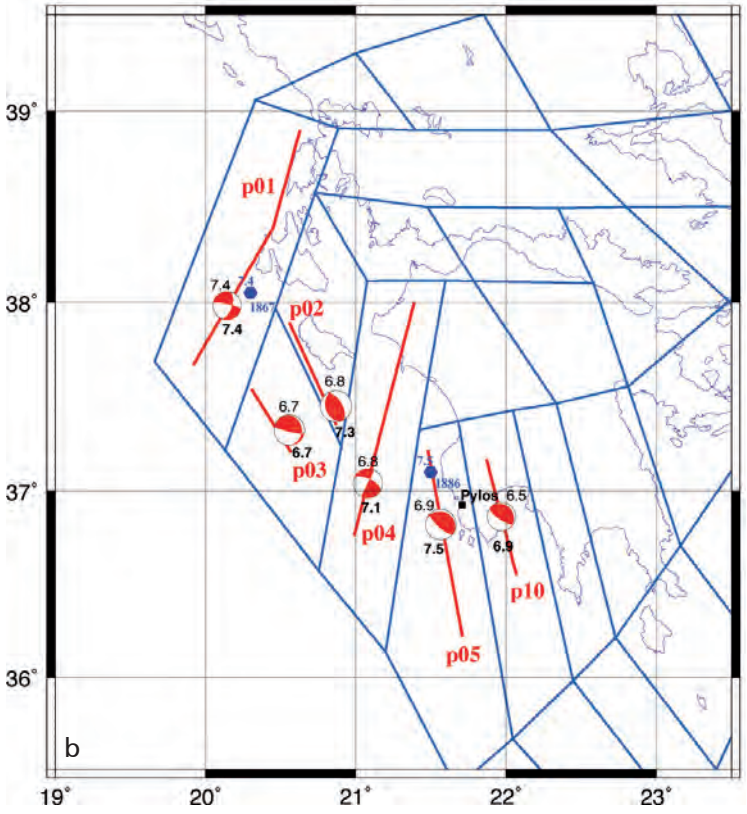

Fig. 17 - SZs of the PYL zonation considered in the PSHA of Pylos, major faults and focal mechanisms in the Pylos broader area: a) fault plane solutions of the main earthquakes in the Ionian Sea, the numbers refer to Table 5; b) events proposed for tsunami generation (see the text for the explanation), the numbers indicate the scenario M_W (M_{dea} and M_{max} of Table 6, the second in bold), the blue diamonds indicate the epicentres of the earthquakes of 1867 and 1886, which generated tsunamis affecting Pylos.

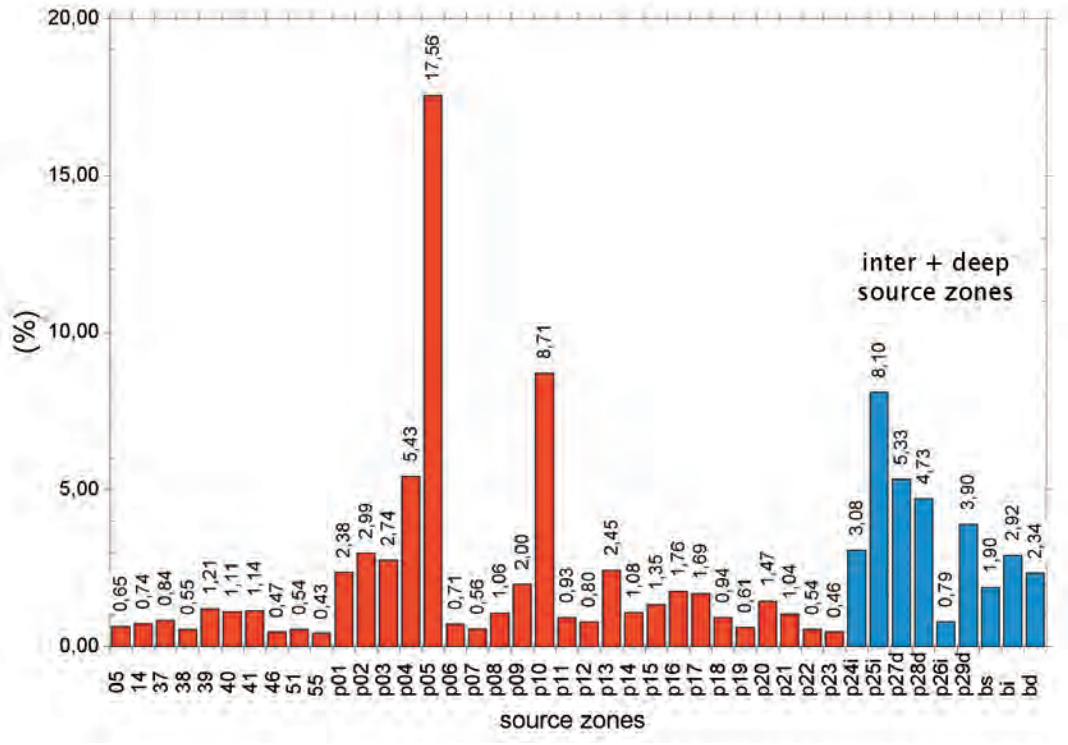

Fig. 18 - Deaggregation for SZs of the seismic hazard results for Pylos related to the 475-year return period: red bars for shallow SZs, blue bars for intermediate and deep SZs.

the SZ because its epicentre is very far from the location of the considered major fault in the SZ. The interpretation of Stiros *et al*. (1995) place the 1953 epicentre in the south-easternmost part of the Cephalonia Island, where also the 1912 event occurred, according to the reported damage (Papazachos and Papazachou, 1997). We consider, then, that these earthquakes can be connected from the seismogenic point of view to SZ p01, rather than to SZ p02. The distance of 120 km and the magnitude of 6.7 identify the bin that contributes most in SZ p03.

5. Scenario earthquakes for tsunami generation in the Ionian Sea

Several tsunamis hit the Ionian coasts in the past. In particular, the village of Pylos suffered twice because of tsunami: in 1867, and 1886. Moreover, it is likely that also the large earthquake of 365, which mostly affected of the Mediterranean area, caused a tsunami in Pylos.

To identify the sources candidate for tsunami generation in the Pylos area (Yalciner *et al*., 2014), the SZs which contribute most to the expected ground motion in Pylos, revealed by the deaggregation analysis, have been studied in details. More precisely, the further deaggregation done in terms of distance and magnitude for the major fault in each of the potentially dangerous SZs has identified the likely locations of future tsunamis. The last step consists in the characterization of the identified seismogenic sources to verify that their rupture mechanism is compatible with a tsunami generation process.

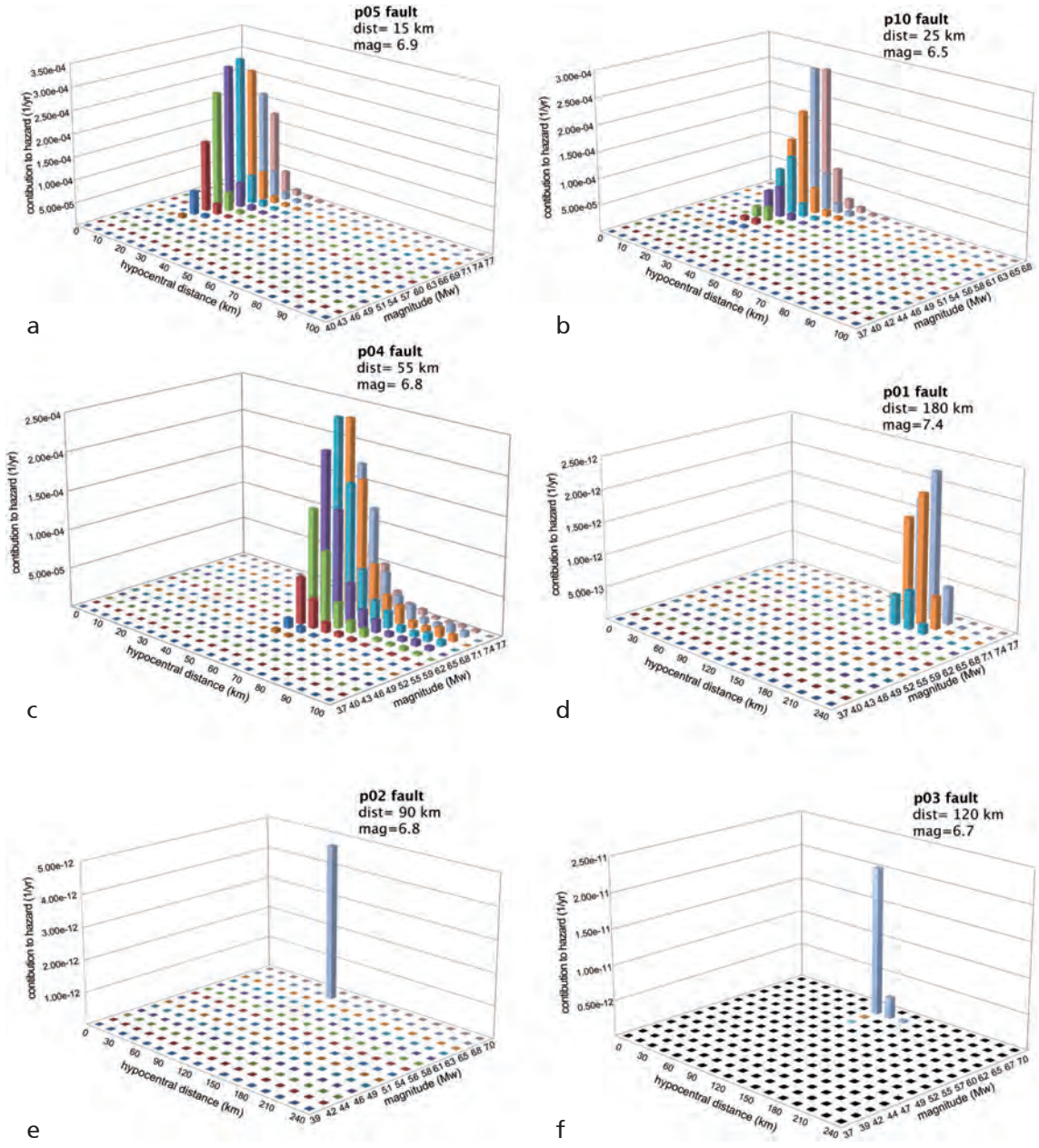

Fig. 19 - Deaggregation for distance and magnitude (considering the major fault in each SZ) of the seismic hazard results for Pylos related to the 475-year return period (see the text for the explanation): a) p05, b) p10, c) p04, d) p01, e) p02, f) p03.

5.2. Focal mechanisms in the Ionian Sea

Table 5 reports and Fig. 17a shows selected focal mechanism of the main earthquakes which occurred in the offshore SZs of the study area. We considered the fault plane solutions contained in three databases: the EMMA database (Vannucci and Gasperini, 2003, 2004), the NOA database (www.gein.noa.gr/index-en.htm), and the CMT one (www.globalcmt.org), with priority accordingly. The selection of the representative mechanisms has been driven by the quality of the

solution: we have given priority to recent events of large magnitude. All the solutions have been checked with other basic studies (e.g., Papazachos *et al.*, 1998).

It can be seen that for both segments of the Cephalonia fault in SZ p01 a similar strike-slip mechanism is available, but the moderate 1973 quake (M_W=5.8) was characterized by a reverse mechanism (n. 7 in Table 5 and Fig. 17a), probably related to a minor offshore thrust. In SZ p02 there is no agreement between the location of the major quake which occurred in 1953 and had an M_W of 6.9 (n. 1 in Table 5 and Fig. 17a), and the location of the major thrust in the SZ (the event n. 4 in Table 5 and Fig. 17a could be associated to its deep prosecution): again the presence of a minor offshore thrust, aligned with the one in SZ p01, can be invoked. Several reverse mechanisms can be roughly associated to the major thrust in SZ p03. It must be pointed out that for thrusts the location of their seismicity is expected far away of the appearance of the fault at the surface, in agreement with the geometry of a gently dipping plane. The strike-slip mechanism of the 2008 earthquake (n. 21 in Table 5 and Fig. 17a) remains associated to the Andravida transcurrent fault, in SZ p04. Again, the presence of a dip-slip mechanism far offshore could be related to the southern continuation of the offshore thrusts of SZs p02 and p03. In SZs p05 and p10 there are 3 reverse mechanisms whose strike fits quite well with the orientation of the 2 thrust faults identified in the SZs. It could be suggested that the 2 thrusts have not a fairly linear geometry, but are formed by segments of slightly different orientation. The presence of a strike-slip event (n. 20 in Table 5 and Fig. 17a) is more problematic in the general geodynamic frame of the region.

5.3. Map of tsunamigenic sources

We have eventually collected all the previous considerations to formulate a hypothesis of scenario earthquakes for tsunami generation. This hypothesis considers the locations obtained by the deaggregation analysis, the geometry of the major fault identified in each SZ, and the mechanism of the main quakes which occurred in the past. Table 6 summaries the scenario earthquakes here proposed. The event geographical coordinates have been derived from the intersection of the fault geometry and the results of the deaggregation. The choice of the distance obtained by the deaggregation analysis is motivated by the fact that this distance, among all those compatible with the fault geometry, contributes more to the hazard in Pylos. The focal depth is that of the quake whose focal mechanism has been selected as representative for the fault, coming from the analysis of Fig. 17a, after a control of its compatibility with the fault style. The magnitudes considered are both the most probable value (M_{dea}) derived from the deaggregation analysis and the geological M_{max}.

Fig. 17b shows the scenario earthquakes proposed for tsunami generation. The coherence between the fault geometry and the focal mechanism is acceptable for almost all cases. The identification of the earthquake whose fault plane solution has been taken as representative of the fault activity can be derived from Table 5 and Fig. 17a.

Entering into details, SZ p01 is characterized by a dextral transcurrent mechanism related to the strike-slip Cephalonia fault. It is, then, not suitable to generate tsunamis although past events showed also a minor vertical motion. Considering the close-by presence of minor thrust earthquakes (e.g., the 1973 event, n. 7 in Table 5 and Fig. 17a), the possibility of a high magnitude (7.4) event, and the close-by presence of the epicentre of the 1867 earthquake, that generated a tsunami interesting Pylos itself, it is reasonable not to exclude this structure as a potential

Table 5 - Selected focal mechanisms for the Ionian Sea. ϕ, δ, and λ are the strike, dip, and rake of the focal mechanism, h is the focal depth in km. RF is the original source of information for the fault plane solution: 1 = Anderson and Jackson (1987), 2 = Papadimitriou (1993), 3 = Baker *et al*. (1997), 4 = Louvari *et al*. (1999), 5 = Kiratzi and Louvari (2003).

N	year	mm	dd	hh	mi	se	Lat N	Lon E	*h*	*Mw*	ϕ	δ	λ	web	RF	zone
1	1953	8	12	09	23	0.0	38.30	20.80	10	6.9	330	57	83	EMMA	1	p02
2	1959	11	15	17	08	40.0	37.80	20.50	12	6.8	46	37	-173	EMMA	2	p02
3	1963	12	16	13	47	53.0	37.00	21.00	7	5.9	296	16	101	EMMA	2	p04
4	1968	3	28	07	39	0.0	37.80	20.90	6	5.9	120	71	64	EMMA	1	p02
5	1969	7	8	08	09	13.0	37.50	20.30	10	5.8	346	13	108	EMMA	3	p03
6	1972	9	17	14	07	15.0	38.30	20.30	8	6.2	45	68	-174	EMMA	2	p01
7	1973	11	4	15	52	14.0	38.89	20.44	23	5.8	324	50	81	EMMA	3	p01
8	1976	5	11	16	59	45.0	37.40	20.40	16	6.3	335	14	106	EMMA	2	p03
9	1976	6	12	00	59	0.0	37.50	20.60	8	5.8	115	70	90	EMMA	1	p03
10	1983	1	17	12	41	31.0	38.10	20.20	11	6.8	39	45	175	EMMA	2	p01
11	1983	3	23	23	51	5.0	38.29	20.26	7	6.1	31	69	174	EMMA	2	p01
12	1987	2	27	23	34	0.0	38.42	20.36	13	5.8	26	61	168	EMMA	4	p01
13	1988	10	16	12	34	13.3	37.95	20.90	29	5.8	301	76	-3	CMT	-	p02
14	1997	10	13	13	39	40.0	36.45	22.16	32	6.3	322	19	108	EMMA	5	p10
15	1997	11	18	13	07	41.0	37.54	20.53	32	6.5	354	20	159	EMMA	5	p03
16	2003	8	14	05	14	54.0	38.82	20.60	12	6.2	18	60	-168	NOA	-	p01
17	2007	3	25	13	58	4.2	38.36	20.24	12	5.7	30	65	164	CMT	-	p01
18	2008	2	14	10	09	22.8	36.55	21.77	25	6.7	290	16	69	NOA	-	p05
19	2008	2	14	12	08	54.8	36.35	21.93	10	6.1	292	18	61	NOA	-	p10
20	2008	2	20	18	27	5.5	36.21	21.71	14	6.0	343	82	-157	NOA	-	p05
21	2008	6	8	12	25	28.4	37.96	21.53	11	6.4	26	89	-152	NOA	-	p04

tsunami generator. The major faults in SZs p02 and p03 are associated with events characterized by thrusting mechanisms and expected moderate magnitude. They should be considered potential generators of moderate tsunamis. SZ p04 is dominated by the transcurrent Andravida fault, whose offshore activity is suggested (but not proved) and the only event associated had a moderate magnitude (6.4) and a strike-slip mechanism. The chance that it can generate tsunamis is not very likely albeit it cannot be excluded. The high M_{max} of the faults identified in SZs p05 and p10, their thrust character, and the presence in SZ p05 of the epicentre of the 1886 earthquake, that generated a tsunami interesting Pylos itself, suggest to consider both structures as possible tsunami generators.

6. Conclusions

Several seismic hazard estimates for the Pylos area have been produced: they refer to the standard return period of 475 years considered in building design and, consequently, can be

Table 6 - Scenario earthquakes for tsunami generation (see the text for the details).

SZ	M_{dea}	M_{max}	Dist. (km)	Lat. N	Lon. E	h (km)	ϕ	δ	λ
p01	7.4	7.4	180	37.96	20.14	12	18	60	-168
p02	6.8	7.3	90	37.45	20.86	10	330	57	83
p03	6.7	6.7	120	37.33	20.54	32	354	20	159
p04	6.8	7.1	55	37.04	21.08	11	26	89	-152
p05	6.9	7.5	15	36.82	21.57	25	290	16	69
p10	6.5	6.9	25	36.86	21.97	32	322	19	108

directly used for seismic hazard zonation purposes. The same estimates have been translated into intensity values (Fig. 16) and, consequently, are suitable for the construction of risk scenarios in terms of expected damage to standard buildings. The results, presented in forms of maps, curves, and UHRSs, for different soil types, give a general picture of the seismic hazard in Pylos and in its surrounding area and are suitable for a seismic risk assessment. In addition, a soil seismic hazard map has been elaborated for the Pylos area.

Pylos is characterized by a high seismic hazard (*PGA* around 0.55 g for a 475-year return period on rock, see Fig. 9a). Such a value is 50% higher than the highest 3rd seismic zone of the Greek seismic code (*PGA* = 0.36 g) though lower than that of the Ionian islands (Cephalonia and Zakynthos, where values between 0.72 and 0.80 g are found, see Fig. 9a). The widespread presence of rock around the town does not suggest the possibility of unexpected high ground motions (see Fig. 12b). It is interesting to note that the influence of the epistemic uncertainty is limited in the Pylos area, where a *PGA* of 0.63 is reached (see Fig. 11). UHRSs computed for Pylos and Zakynthos (Fig. 14) clearly point out the different level of expected ground shaking in the two sites.

The results obtained for Pylos in the present study (0.55 g for a return period of 475 years) are identical to those (0.56 g) already obtained by SEAHELLARC Working Group (2010) and in full agreement with the estimates obtained by Weatherill and Burton (2010): 0.4 to 0.5 g for the western coast of Peloponnese. The present results are remarkably higher than those available in literature [0.143 for Makropoulos and Burton (1985) and 0.29 for Papazachos *et al*. (1993)]. It must be pinpointed that the former authors did not consider the aleatory uncertainty of the GMPE and it is not clear whether the latter ones introduced it, or not, in their computation (no standard deviation was indicated for the GMPEs applied). Furthermore, the value given by Papazachos *et al*. (1993) is an average estimate because it refers to the entire south-western coast of the Peloponnese. Moreover, Papaioannou and Papazachos (2000) estimated an intensity of VII-VIII MM for the same return period of 475 years for Pylos. Considering the scaling laws of Koliopoulos *et al*. (1998) and of Tselenis and Danciu (2008), we obtain mean values of 0.27 and 0.24 g, respectively. Again, it is not clear if the standard deviation of the GMPE was considered in these computations (we have not taken into account the uncertainty of intensity vs. *PGA* scaling laws cited above). As already pointed out by SEAHELLARC Working Group (2010), re-computing the expected ground motion in Pylos, according to the input data (zonation, seismicity rates, and attenuation model without standard deviation) provided by Papaioannou and Papazachos (2000), a value of 0.24 g is obtained for a return period of 475 years: such value

is in full agreement with the literature results, suggesting that a fully probabilistic approach was not followed in the past.

Moreover, a suite of possible tsunamigenic sources in the Ionian Sea, in terms of location, magnitude, and mechanism, has been identified (see Fig. 17b): it represents the basic information for tsunami modelling. A total of 5 out of the 6 identified faults located offshore the western coast of the Peloponnese show characteristics that suggest the possibility that they can generate tsunamis affecting Pylos town.

Acknowledgements. The earthquake data used in the elaborations have been provided by Gerassimos Papadopoulos and his colleagues of the University of Athens. The identification of the main seismogenic sources was developed in co-operation with Rinaldo Nicolich of the University of Trieste. Several figures have been produced using the Generic Mapping Tool (GMT) software package (Wessel and Smith, 1991). Many thanks are due to Eleftheria Papadimitriou and an anonymous reviewer for useful comments and suggestions that have improved the text.

REFERENCES

Abrahamson N.A. and Bommer J.J.; 2005: *Probability and uncertainty in seismic hazard analysis*. Earthquake Spectra, **21**, 603-607.

Albarello D. and Mucciarelli M.; 2002: *Seismic hazard estimates using ill-defined macroseismic data at site*. Pure Appl. Geophys., **159**, 1289-1304.

Albarello D., Bosi, V., Bramerini F., Lucantoni A., Naso G., Peruzza L., Rebez A., Sabetta F., Slejko D.; 2000: *Carte di pericolosità sismica del territorio nazionale*. Quaderni di Geofisica, **12**, 1-7.

Ambraseys N.N.; 1995: *The prediction of earthquake peak ground acceleration in Europe*. Earthquake Eng. Struct. Dyn., **24**, 467-490.

Ambraseys N.N.; 2003: *Reappraisal of magnitude of 20th century earthquakes in Switzerland*. J. Earthquake Engineering, **7**, 149-191.

Ambraseys N.N., Simpson K.A. and Bommer J.J.; 1996: *Prediction of horizontal response spectra in Europe*. Earth. Eng. Struct. Dyn., **25**, 371-400.

Anderson H. and Jackson, J., 1987: *Active tectonics of the Adriatic region*. Geophys. J. R. Astr. Soc., **91**, 937 - 983.

Arias A.; 1970: *A measure of earthquake intensity*. In: Hansen R.J. (ed), Seismic design of nuclear power plants, M.I.T. Press, Cambridge, pp. 438-483.

Atkinson G.M. and Boore D.M.; 2003: *Empirical ground-motion relations for subduction-zone earthquakes and their application to Cascadia and other regions*. Bull. Seism. Soc. Am., **93**, 1703-1729.

Baker C., Hatzfeld D., Lyon-Caen H., Papadimitriou E. and Rigo A.; 1997: *Earthquake mechanisms of the Adriatic Sea and Western Greece: implications for the oceanic subduction-continental collision transition*. Geoph. J. Int., **131**, 559-594.

Bazzurro P. and Cornell C.A.; 1999: *Disaggregation of seismic hazard*. Bull. Seism. Soc. Am., **89**, 501-520.

CEN (Comité Européen de Normalisation); 2002: *Eurocode 8: design of structures for earthquake resistance*. *Part 1: general rules, seismic actions and rules for buildings*. Draft No 5, Doc CEN/T250/SC8/N317, CEN, Brussels, 100 pp.

Coppersmith K.J. and Youngs R.R.; 1986: *Capturing uncertainty in probabilistic seismic hazard assessments within intraplate environments*. In: Proceedings of the Third U.S. National Conference on Earthquake Engineering, August 24-28, 1986, Charleston, SC, Earthquake Engineering Research Institute, El Cerrito CA U.S.A., vol. 1, pp 301-312.

Cornell C.A.; 1968: *Engineering seismic risk analysis*. Bull. Seism. Soc. Am., **58**, 1583-1606.

Cramer C.H., Wheeler R.L. and Mueller C.S.; 2002: *Uncertainty analysis for seismic hazard in the southern Illinois basin*. Seism. Res. Lett., **73**, 792-805.

Danciu L. and Tselensis G.-A.; 2007: *Engineering ground-motion parameters attenuation relationships for Greece*. Bull. Seism. Soc. Am., **97**, 162-183.

Gardner J.K. and Knopoff L.; 1974: *Is the sequence of earthquakes in southern California, with aftershocks removed, Poissonian?* Bull. Seism. Soc. Am., **64**, 1363-1367.

IGME (Institute of Geology and Mineral Exploration); 1980: *Koroni-Pylos-Skhiza sheet*. Geological map of Greece, I.G.M.E., Athens.

Joyner W. B. and Boore D. M.; 1981: *Peak horizontal acceleration and velocity from strong-motion records including records from the 1979 Imperial Valley, California, earthquake*. Bull. Seism. Soc. Am., **71**, 2011-2038.

Kijko A. and Graham G.; 1998: *Parametric-historic procedure for probabilistic seismic hazard analysis. Part I: estimation of maximum regional magnitude* m_{max}. Pure Appl. Geophys., **152**, 413-442.

Kiratzi A. and Louvari E.; 2003: *Focal mechanisms of shallow earthquakes in the Aegean Sea and the surrounding lands determined by waveform modelling: a new database*. Journal of Geodynamics, **36**, 251–274.

Koliopoulos P.K., Margaris B.N. and Klimis N.S.; 1998: *Duration and energy characteristics of Greek strong motion records*. J. Earth. Eng., **2**, 391-417.

Kulkarni R.B., Youngs R.R. and Coppersmith K.J.; 1984: *Assessment of confidence intervals for results of seismic hazard analysis*. In: Proceedings of the Eighth World Conference on Earthquake Engineering, July 21-28, 1984, San Francisco CA U.S.A., Prentice-Hall Inc., Englewood Cliffs NJ U.S.A., Vol 1, pp 263-270.

Latoussakis J. and Stavrakakis G.N.; 1992: *Times of increased probability of earthquakes of ML ≥ 5.5 in Greece diagnosed by algorithm M8*. Tectonophysics, **210**, 315-326.

Louvari E. K., Kiratzi A. A. and Papazachos B. C.; 1999: *The Cephalonia transform fault and its extension to western Lefkada island (Greece)*. Tectonophysics, **308**, 223-236.

Makropoulos K.C. and Burton P.W.; 1985: *Seismic hazard in Greece. II. Ground acceleration*. Tectonophysics, 117, 259-294.

Mark R.K.; 1977: *Application of linear statistical model of earthquake magnitude versus fault length in estimating maximum expectable earthquakes*. Geology, **5**, 464-466.

McClusky S., Balassanian S., Barka A., Demir C., Ergintav S., Georgiev I., Gurkan O., Hamburger M., Hurst K., Kahle H., Kastens K., Kekilidze G., King R., Kotzev V., Lenk O., Mahmoud S., Mishin A., Nadariya M., Ozounis A., Paradissis D., Peter Y., Prelipin M., Reilinger R., Sanli I., Seeger H., Tealeb A., Toksöz M.N. and Veis G.; 2000: *Global Positioning System constraints on plate kinematics and dynamics in the eastern Mediterranean and Caucasus*. J. Geophys. Res., **105**, 5695–5719.

McGuire R.K.; 1977: *Effects of uncertainties in seismicity on estimates of seismic hazard for the east coast of the United States*. Bull. Seism. Soc. Am., **67**, 827-848.

McGuire R.K.; 2005: *The case of using mean seismic hazard*. Earthquake Spectra, **21**, 879-886.

McGuire R.K. and Shedlock K.M.; 1981: *Statistical uncertainties in seismic hazard evaluations in the United States*. Bull. Seism. Soc. Am., **71**, 1287-1308.

Musson R.M.W.; 2005: *Against fractiles*. Earthquake Spectra, **21**, 887-891.

Ordaz M., Aguilar A. and Arboleda J.; 2007: *CRISIS 2007 Program for computing seismic hazard*. Vers. 1.1. UNAM, Mexico.

Ordaz M., Faccioli E., Martinelli F., Aguilar A., Arboleda J., Meletti C. and D'Amico V.; 2012: *CRISIS 2012 Program for computing seismic hazard*. Vers. 4.2. UNAM, Mexico.

Papadimitriou E.E.; 1993: *Focal mechanism along the convex side of the Hellenic arc*. Boll. Geof. Teor. Appl., **35**, 401-426.

Papadopoulos G.A. and Plessa A.; 2001: *Historical earrthquakes and tsunamis of the South Ionian Sea occurring from 1591 to 1837*. Bull. Geol. Soc. Greece, **34**, 1547-1554.

Papadopoulos G.A. and Vassilopoulou A.; 2001: *Historical and archaeological evidence of earthquakes and tsunamis felt in the Kythira strait, Greece*. In: Hebenstreit G.T. (ed), Tsunami Research at the End of a Critical Decade, Kluwer, pp. 119-138.

Papadopoulos G.A., Vassilopoulou A. and Plessa A.; 2000: *A new catalogue of historical earthquakes in the Corinth Rift, Central Greece: 480B.C. – A.D. 1910*. In: Papadopoulos G.A. (ed), Historical Earthquakes and Tsunamis in the Corinth Rift, Central Greece, Inst. of Geodynamics, Natl. Observatory of Athens, Publ. No 12, pp. 9-119.

Papadopoulos G.A., Daskalaki E., Fokaefs A. and Giraleas N.; 2010: *Tsunami hazard in the Eastern Mediterranean sea: strong earthquakes and tsunamis in the west Hellenic arc and trench system*. J. of Earthquakes and Tsunami, **4**, 145-179.

Papadopoulos G.A., Fokaefs A. and Baskoutas I.; 2014: *Historical seismicity of the Kyparissiakos Gulf, western Peloponnese, Greece*. Boll. Geof. Teor., Appl., **55**, xx-xx, doi: 10.4430/bgta0096.

Papaioannou Ch.A. and Papazachos B.C.; 2000: *Time-independent and time-dependent seismic hazard in Greece based on seismogenic sources*. Bull. Seism. Soc. Am., **90**, 22-33.

Papazachos B.C. and Papazachou C.B.; 1997: *The earthquakes of Greece*. Ziti Publications, Thessaloniki, 304 pp.

Papazachos B.C., Papaioannou Ch.A., Margaris B.N. and Theodulidis N.P.; 1993: *Regionalization of seismic hazard in Greece based on seismic sources*. Natural Hazards, **8**, 1-18.

Papazachos B.C., Papadimitriou E.E., Kiratzi A.A., Papazachos C.B. and Louvari E.K.; 1998: *Fault plane solutions in the Aegean Sea and the surrounding area and their tectonic implications*. Boll. Geof. Teor. Appl., **39**, 199-218.

Papazachos B.C., Comninakis P.E., Karakaisis G.F., Karakostas B.G., Papaioannou Ch.A., Papazachos C.B. and Scordilis E.M.; 2000a: *A catalogue of earthquakes in Greece and surrounding area for the period 550BC-1999*. Publ. Geoph. Lab., Univ. of Thessaloniki, 1, 333 pp., available at http://geophysics.geo.auth.gr/ss/catalogs_en.html.

Papazachos B.C., Karakostas V.G., Papazachos C.B. and Scordilis E.M.; 2000b: *The geometry of the Wadati – Benioff zone and lithosheric Kinematics in the Hellenic arc*. Tectonophysics, **319**, 275-300.

Papazachos B.C., Karakostas V.G., Kiratzi A.A., Margaris B.N., Papazachos C.B. and Scordilis E.M.; 2002: *Uncertainties in the estimation of earthquake magnitudes in Greece*. J. Seismol., **6**, 557-570.

Papoulia J.E. and Slejko D.; 1997: *Seismic hazard assessment in the Ionian islands based on observed macroseismic intensities*. Natural Hazards, **14**, 179-187.

Papoulia J., Makris J., Mascle J., Slejko D. and Yalçiner A.; 2014: *The EU SEAHELLARC project: aims and main results*. Boll. Geof. Teor. Appl., **55**, 241-248, doi: 10.4430/bgta 0100.

Pavlides S. and Caputo R.; 2004: *Magnitude versus faults' surface parameters: quantitative relationships from the Aegean region*. Tectonophysics, **380**, 159-188.

Pomonis A. and Gaspari M.; 2014: *Earthquake loss estimation and benefit-cost analysis of mitigation measures for buildings in Greece: case study of Pylos town*. Boll. Geof. Teor. Appl., **55**, 535-560, doi: 10.4430/bgta 0072.

Rebez A. and Slejko D.; 2004: *Introducing epistemic uncertainties into seismic hazard assessment for the broader Vittorio Veneto area (N.E. Italy)*. Boll. Geof. Teor. Appl., **45**, 305-320.

Reiter L.; 1990: *Earthquake hazard analysis: issues and insights*. Columbia University Press, New York, 252 pp.

Schmidt Diaz V.; 2008: *Correlaciones a partir de la intensidad de Arias para datos acelerograficos de Costa Rica*. Rev. Geol. Am. Centr., **38**, 95-117.

Schwartz D.P and Coppersmith K.J.; 1984: *Fault behavior and characteristic earthquakes: examples from the Wasatch and San Andreas fault zones*. J. Geophys. Res., **89**, 5681-5698.

Scordilis E.M., Karakaisis G.F., Karacostas B.G., Panagiotopoulos D.G., Comninakis P.E. and Papazachos B.C.; 1985: *Evidence for transform faulting in the Ioanian Sea: the Cephalonia Island earthquake sequence of 1983*. PAGEOPH, **123**, 388-397.

SEAHELLARC Working Group; 2010: *Preliminary seismic hazard assessments for the area of Pylos and surrounding region (SW Peloponnese)*. Boll. Geof. Teor. Appl., **51**, 163-186.

SEAHELLARC Working Group; 2014: *A new seismogenic model for the Kyparissiakos Gulf and western Peloponnese (SW Hellenic Arc)*. Boll. Geof. Teor. Appl., **55**, 405-432, doi: 10.4430/bgta 0127.

Skarlatoudis A.A., Papazachos C.B., Margaris B.N., Theodulidis N., Papaioannou C., Kalogeras I., Scordilis E.M. and Karakostas V.; 2003: *Empirical peak ground-motion predictive relations for shallow earthquake in Greece*. Bull. Seism. Soc. Am., **93**, 2591–2603.

Slejko D. and Rebez A.; 2002: *Probabilistic seismic hazard assessment and deterministic ground shaking scenarios for Vittorio Veneto (N.E. Italy)*. Boll Geof. Teor. Appl., **43**, 263-280.

Slejko D., Peruzza L. and Rebez A.; 1998: *Seismic hazard maps of Italy*. Annali di Geofisica, **41**, 183 - 214.

SSHAC (Senior Seismic Hazard Analysis Committee); 1997: *Recommendations for probabilistic seismic hazard analysis: guidance on uncertainty and use of experts*. NUREG/CR-6372, Lawrence Livermore Nat. Lab., Livermore, 256 pp.

Stiros S.C., Pirazzoli P.A., Laborel J. and Laborel-Deguen F.; 1995: *The 1953 earthquake in Cephalonia (western Hellenic Arc): coastal uplift and halotectonic faulting*. Geoph. J. Int., **117**, 834-849

Toro G.R., Abrahamson N.A. and Schneider J.F.; 1997: *Model of strong motions from earthquakes in central and eastern North America: best estimates and uncertainties*. Seism. Res. Lett., **68**, 41-57.

Tselenstis G.-A. and Danciu L.; 2008: *Empirical relationships between Modified Mercalli intensity and engineering ground-motion parameters in Greece*. Bull. Seism. Soc. Am., **98**, 1863-1875.

Vannucci G. and Gasperini P.; 2003: *A database of revised fault plane solutions for Italy and surrounding regions*. Computers & Geosciences, **29**, 903-909.

Vannucci G. and Gasperini P.; 2004: *The new release of the database of Earthquake Mechanisms of the Mediterranean Area (EMMA version 2)*. Annals of Geophysics, Supplement to Vol. **47**, 303-327.

Vlastos S., Papadimitriou E., Papazachos C. and Karakostas V.; 2002: *Determination of seismic lineaments in the Aegean area and deformation velocities*. In: 11th General Assembly of the Wegener Project, Athens June 12-14, 2002.

Weatherill G. and Burton P.W.; 2010: *An alternative approach to probabilistic seismic hazard analysis in the Aegean region using Monte Carlo simulation*. Tectonophysics, **492**, 253-278, doi:10.1016/j.tecto.2010.06.022

Wells D.L. and Coppersmith K.J.; 1994: *New empirical relationship among magnitude, rupture length, rupture width, rupture area, and surface displacement*. Bull. Seism. Soc. Am., **84**, 974-1002.

Wessel P. and Smith W.; 1991: *Free software helps map and display data*. EOS Trans AGU, **72**, 441–461.

Yalçiner A.C., Gülkan P., Dilmen D.I., Aytore B., Ayca A., Insel I. and Zaytsev A.; 2014: *Evaluation of tsunami scenario in western Peloponnese, Greece*. Boll. Geof. Teor. Appl., **55**, 485-500, doi: 10.4430/bgta 0126.

Youngs R.R., Chiou S.-J., Silva W.J. and Humphrey J.R.; 1997: *Strong ground motion attenuation relationships for subduction zone earthquakes*. Seism. Res. Letts, **68**, 58-73.

Corresponding author: Dario Slejko
Istituto Nazionale di Oceanografia e di Geofisica Sperimentale
Borgo Grotta Gigante 42c, 34010 Sgonico (TS), Italy
Phone: +39 040 2140248; fax: +39 040 327307; e-mail: dslejko@inogs.it